

On the foundations and extremal structure of the holographic entropy cone *

David Avis

School of Informatics, Kyoto University, Kyoto, Japan and
School of Computer Science, McGill University, Montréal, Québec, Canada

Sergio Hernández-Cuenca

Center for Theoretical Physics, Massachusetts Institute of Technology, Cambridge, MA, USA

December 7, 2022

Abstract

The holographic entropy cone (HEC) is a polyhedral cone first introduced in the study of a class of quantum entropy inequalities. It admits a graph-theoretic description in terms of minimum cuts in weighted graphs, a characterization which naturally generalizes the cut function for complete graphs. Unfortunately, no complete facet or extreme-ray representation of the HEC is known. In this work, starting from a purely graph-theoretic perspective, we develop a theoretical and computational foundation for the HEC. The paper is self-contained, giving new proofs of known results and proving several new results as well. These are also used to develop two systematic approaches for finding the facets and extreme rays of the HEC, which we illustrate by recomputing the HEC on 5 terminals and improving its graph description. We also report on some partial results for 6 terminals. Some interesting open problems are stated throughout.

Keywords: holographic entropy cone, polyhedral computation, cut functions, extreme rays, facets, entropy inequalities, quantum information

Contents

1	Introduction	2
2	Definitions and basic results	3
2.1	Polyhedrality of the HEC	5
2.2	Representations of the HEC	8
3	Extreme rays	10
3.1	A lifting of the HEC	10
3.2	Zero-lifting extreme rays	12
4	Valid inequalities and facets	14
4.1	Proof by contraction	15
4.2	Zero-lifting of valid inequalities and facets	18

*DA was supported by JSPS Kakenhi Grants 16H02785, 18H05291 and 20H00579.
SHC was supported by NSF Grant PHY-1801805 and the University of California, Santa Barbara.

5	Integer programs for testing realizability and validity	21
6	Computing H- and V-representations of H_n	23
6.1	Method 1	23
6.2	Method 2	25
6.3	Comparison of Method 1 and Method 2	26
7	Conclusion	27
A	Origins and importance of the HEC in physics	29
B	Extremal structure of H_n for $1 \leq n \leq 5$	30
B.1	Facets	30
B.2	Extreme rays and minimum graph realizations	31
C	Miscellaneous examples	33

1 Introduction

The holographic entropy cone (HEC) has its origins in quantum physics in the work of Bao et al. [1] as described briefly in Appendix A. The HEC is a family of polyhedral cones $H_n, n \geq 1$. A crucial result of their paper is a graph-theoretic characterization in terms of minimum cuts in a complete graph, which is a natural generalization of the well-studied cone of cut functions. This allows us to study the HEC without any reference to the underlying quantum physics setting. Apart from its relationship to cut functions, the HEC does not appear to be related to other known polyhedral objects. Our main focus is on the extremal structure of the HEC. At present no compact representation of either the extreme rays or the facets of H_n is known and a complete explicit description is only known up to $n = 5$, see [1, 14]. The main motivation for studying the extremal structure of the HEC is the characterization of its facets, which physically correspond to entropy inequalities that strongly constrain the entanglement patterns of quantum states encoding higher-dimensional spacetimes as their quantum gravity duals in holography [1, 5] – see Appendix A for more details

This paper is structured as follows. Firstly, in Section 2 we give a formal definition of H_n and some basic structural results that will be needed throughout the paper. These include new proofs that it is full-dimensional and polyhedral. In proving the latter result, using antichains in a lattice, we obtain a tighter bound on the size of the complete graph needed to realize all extreme rays of H_n . We then review some basic results on the H - and V -representations of cones and study H_2 relating it to the cone of cut functions. In Section 3 we discuss the extreme rays of H_n and describe some related cones that lead to methods to compute them. This gives a simple proof that the H_n is a rational cone. It also allows us to give a description of H_3 . Following that we give a general zero-lifting result for extreme rays. In Section 4 we describe valid inequalities and facets. We begin by reviewing the proof-by-contraction method that is used for proving validity of inequalities. In the proof we again use antichains, obtaining a reduction in the complexity of the original method. This is followed by a discussion of zero-lifting of valid inequalities and facets. In Section 5 we describe integer programs that can be used to test membership in H_n and prove non-validity of inequalities defined over it. Many of the results of the paper are combined in Section 6, which describes two methods to derive complete facet and extreme-ray descriptions of H_n and illustrate these on computations of H_5 . There are a lot of interesting open problems related to the HEC, and some of these are stated throughout the paper and in the conclusion. Supplemental material, including input and output

files, integer linear programs and C code for various functions mentioned, is available online¹.

2 Definitions and basic results

For any positive integers k and N , let $[k] = \{1, 2, \dots, k\}$, and let K_N denote the undirected complete graph on the vertex set $[N]$. The edge set E_N consists of all edges $e = (i, j)$ between vertices $i, j \in [N]$ for every pair $1 \leq i < j \leq N$. A weight map $w : E_N \rightarrow \mathbb{R}_{\geq 0}$ is introduced to assign a nonnegative weight $w(e)$ to every $e \in E_N$. Any subset $W \subseteq [N]$ defines a *cut* $C(W)$ as the set of all edges (i, j) with $i \in W$ and $j \notin W$. Since both W and its complement define the same cut, we will normally consider cuts where $W \subseteq [N - 1]$, and generally exclude the empty cut. We denote by $S_W = \|C(W)\|$ the total weight of the cut $C(W)$, which is the sum of the weights of all the edges in $C(W)$. Letting $n = N - 1$, consider the *S-vector* of length $2^n - 1$ with entries indexed by cardinality and then lexicographically by the non-empty subsets of $[n]$,

$$S = (S_1, S_2, \dots, S_n, S_{12}, \dots, S_{12\dots n}), \quad (2.1)$$

where juxtaposition is a shorthand for the corresponding set of integers. The convex hull of the set of all S vectors for a given N forms a cone in $\mathbb{R}^{2^n - 1}$. In fact, this cone is polyhedral, its facets are the subadditivity inequalities and the submodular inequalities are valid for it, as established independently by Tomizawa and Fujishige (see Section 3.6 of [11]) and Cunningham [6]. When the vector S is expressed as a function of W it is known as the *cut function*.

The HEC is a generalization of the cone defined by the cut function. We follow [1], but adapt its notation and terminology considerably. Instead of setting $n = N - 1$, we fix some integer $n \geq 2$ and consider K_N for all $N > n$. In any such graph, we call the vertices $[n]$ *terminals* (cf. boundary regions in holography). The vertex N is called the *purifying vertex* in the physics literature, but we will simply call it the *sink* here. Oftentimes, these will be combined into $[n; N] = [n] \cup \{N\}$ and collectively referred to as *extended terminals*. The other vertices, if any, are called *bulk* vertices (cf. the bulk spacetime).

Let I be a non-empty subset of terminals, i.e. $\emptyset \neq I \subseteq [n]$. We extend the definition of S above to this new setting. For any $N > n$ and weight map w defined on K_N , we introduce a construct which captures all the basic properties conveyed by the RT formula in (A.1). In particular, let

$$S_I = \min_{I=W \cap [n]} \|C(W)\|, \quad (2.2)$$

where the minimization is over all $W \subseteq [N - 1]$. This says that S_I takes the minimum weight over all cuts which contain precisely the terminals in I and some (possibly empty) subset of the bulk vertices. Note that when $n = N - 1$ we are minimizing over the single subset $W = I$ and the definition is equivalent to the one given earlier. In graph theory terms, S_I is just the capacity of the minimum-weight cut or *min-cut* in K_N separating I from $[n; N] \setminus I$. By the duality of cuts and flows, an equivalent definition is to let S_I be the value of the maximum flow between multiple-sources I and multiple-sinks $[n; N] \setminus I$ in K_N . The max flow problems are structurally different for each I but nevertheless give an efficient method of computing the S_I .

We form an S -vector from (2.2) of the form of (2.1) as we did previously, and say that w *realizes* S in K_N or, more compactly, that (S, w) is a *valid pair*.

Definition 1. The *holographic entropy cone* on n terminals is defined as

$$H_n = \{S \in \mathbb{R}^{2^n - 1} : (S, w) \text{ is a valid pair for some } N \text{ and } w\}. \quad (2.3)$$

¹<http://cgm.cs.mcgill.ca/~avis/doc/HEC/HEC.html>

Examples of the facet defining inequalities and extreme rays of H_n for small n are given in Appendices B.1 and B.2 respectively.

It follows from (2.2) that for any $\lambda > 0$, (S, w) is a valid pair for H_n if and only if $(\lambda S, \lambda w)$ is, so H_n is a cone. In fact it is full-dimensional. The proof employs S -vectors arising from K_{n+2} with all edges of zero weight except possibly edges $(i, n+1)$ for $i \in [n; N]$. We call these *star graphs* and exhibit a family of $2^n - 1$ of them giving linearly independent S -vectors.

Proposition 1. H_n is a cone of dimension $2^n - 1$.

Proof. For each $\emptyset \neq J \subseteq [n]$, define a weighted star graph where the nonzero edge weights are²

$$w_i = 1, \quad \forall i \in J \quad \text{and} \quad w_N = \begin{cases} 1 & \text{if } |J| = 1, \\ |J| - 1 & \text{otherwise.} \end{cases} \quad (2.4)$$

For every $n \geq 2$, their respective S -vectors S^J can be easily seen to be given by

$$S_I^J = |I \cap J| - \delta(I, J), \quad \delta(I, J) = \begin{cases} 1 & \text{if } |J| \geq 2 \text{ and } I \supseteq J, \\ 0 & \text{otherwise.} \end{cases} \quad (2.5)$$

Using them as row vectors, we construct square matrices A^n . For example,

$$A^2 = \begin{array}{c} \begin{array}{ccc|c} \sphericalangle & \sphericalangle & \sphericalangle & \\ \hline 1 & 1 & 0 & 1 \\ 1 & 1 & 1 & 12 \\ 0 & 1 & 1 & 2 \end{array} \\ \dots \\ A^{n+1} = \begin{array}{c} \begin{array}{ccc|ccc} \sphericalangle & \\ \hline 1 & 0 & 1 & 1 & 0 & 1 & 0 & 1 \\ 0 & 1 & 1 & 0 & 1 & 1 & 0 & 2 \\ 1 & 1 & 1 & 1 & 1 & 1 & 0 & 12 \\ \color{red}{1} & 0 & 1 & \color{red}{1} & \color{red}{1} & \color{red}{1} & 1 & 13 \\ \color{blue}{0} & \color{red}{1} & 1 & \color{blue}{1} & \color{red}{1} & \color{red}{1} & 1 & 23 \\ \color{red}{1} & \color{blue}{1} & \color{red}{2} & \color{blue}{2} & \color{red}{2} & \color{red}{2} & 1 & 123 \\ \hline 0 & 0 & 0 & 1 & 1 & 1 & 1 & 3 \end{array} \end{array} \begin{array}{c} \begin{array}{c} I \\ I \cup \{n+1\} \\ \{n+1\} \end{array} \\ \begin{array}{c} B^n \\ C^n \\ D^n \\ d \end{array} \quad \begin{array}{c} C^n \\ E^n \\ \vdots \\ \dots \end{array} \quad \begin{array}{c} c \\ \vdots \\ \cdot \end{array} \quad \begin{array}{c} J \\ J \cup \{n+1\} \\ \{n+1\} \end{array} \end{array} \quad (2.6)$$

where the general sketch partitions A^{n+1} into four square matrices B^n , C^n , D^n and E^n , of size $2^n - 1$, a final column c , and a final row d . Note that the rows and columns have been permuted from their usual ordering for subsets of $[n+1]$. Here, labels $\emptyset \neq I \subseteq [n]$ go first, then those of the form $I \cup \{n+1\}$, and $\{n+1\}$ last (cf. the block forms in (2.6)). We prove by induction on n that $\det(A^n) = (-1)^{n+1}$. This is immediate for $n = 2$. Matrix B^n in A^{n+1} is just A^n reordered as described above. Since we perform the same reordering for rows as for columns the determinant sign is unchanged, so by the induction hypothesis $\det(B^n) = (-1)^{n+1}$. As the rows of B^n and C^n are indexed by $J \not\ni n+1$, we have $C^n = B^n$. Additionally, one easily verifies that in c the first $2^n - 1$ entries are 0 and the rest are 1. Row d has the same pattern.

We now make a comparison between entries in column $I \not\ni n+1$ of D^n and column $I \cup \{n+1\}$ of E^n . Consider the diagonal elements of each. For row J , in D^n we have column $I = J \setminus \{n+1\}$ and so $S_I^J = |I| = |J| - 1$. In E^n the column label is also J and since $|J| \geq 2$ we have $\delta(I, J) = 1$ and so $S_I^J = |J| - 1$. Hence the diagonals are identical. Now consider the elements below them. For D^n each row index J contains $n+1$ but none of its column indices do, so $S_I^J = |I \cap J|$.

²This class of star graphs were inspired by a construction of [18].

In E^n the same applies but the intersection now includes $n + 1$, so the corresponding entry is always bigger by one. These facts are illustrated by the coloured entries in A^3 .

We now subtract the first $2^n - 1$ columns of A^{n+1} from the next $2^n - 1$ columns, then subtract c from each of these columns also, obtaining

$$A^{n+1} = \begin{bmatrix} B^n & B^n & \mathbf{0} \\ D^n & E^n & \mathbf{1} \\ \mathbf{0} & \mathbf{1} & 1 \end{bmatrix} \quad \longrightarrow \quad \tilde{A}^{n+1} = \begin{bmatrix} B^n & \mathbf{0} & \mathbf{0} \\ D^n & E^n - D^n - \mathbf{1} & \mathbf{1} \\ \mathbf{0} & \mathbf{0} & 1 \end{bmatrix}. \quad (2.7)$$

Here $\mathbf{0}$ and $\mathbf{1}$ respectively denote all-0 or all-1 matrices of suitable size. In the resulting \tilde{A}^{n+1} , notice that $E^n - D^n - \mathbf{1}$ is an upper triangular matrix with all diagonal elements equal to -1 . Recalling that $\det(B^n) = (-1)^{n+1}$, we have $\det(A^{n+1}) = \det(\tilde{A}^{n+1}) = (-1)^{n+2}$, as desired. \square

We will show in the following sections that H_n is also convex, polyhedral and rational. One important basic property the S -vectors do not possess is monotonicity, as can be seen by examples in Appendix B.2.

2.1 Polyhedrality of the HEC

The polyhedrality of the HEC was established by Bao et al. [1]. We give a proof of this crucial result here following similar lines to the original proof but obtain a tighter result due to our use of antichains. In general, there may be more than one min-cut W for each $\emptyset \neq I \subseteq [n]$ achieving the minimum in (2.2). Among these, let W_I denote one which is minimal under set inclusion. We call W_I a *minimal min-cut* for I and have $S_I = \|C(W_I)\|$. The following basic theorem shows that these are unique and builds on results from Lemma 6 of [20], and Theorems 3.1 and 3.2 of [2].

Theorem 1. *For positive integers $n < N$, consider a weighted complete graph K_N with terminal set $[n]$. Let W_I and W_J be minimal min-cuts for $\emptyset \neq I, J \subseteq [n]$. Then:*

- (a) *Each $I \subseteq [n]$ has a unique minimal min-cut W_I .*
- (b) $I \subseteq J \iff W_I \subseteq W_J$.
- (c) $I \cap J = \emptyset \iff W_I \cap W_J = \emptyset$.
- (d) *If $m = \left| \bigcup_{I \subseteq [n]} W_I \right|$, then all minimal min-cuts can be represented in a weighted K_{m+1} .*

Proof.

- (a) Suppose W and W' are minimal min-cuts for I . Submodularity of the cut function gives

$$\|C(W)\| + \|C(W')\| \geq \|C(W \cup W')\| + \|C(W \cap W')\|. \quad (2.8)$$

Clearly, $W \cup W'$ and $W \cap W'$ are cuts for I . Since W and W' are additionally min-cuts,

$$\|C(W \cup W')\| \geq \|C(W)\|, \quad \|C(W \cap W')\| \geq \|C(W')\|, \quad (2.9)$$

thereby turning all inequalities above into equations. Hence $W \cap W'$ is a min-cut and, as an intersection of minimal ones, minimal as well. It must thus be the case that $W = W' = W_I$.

(b) First assume that $W_I \subseteq W_J$. Since W_I and W_J are cuts for I and J respectively, we have $W_I \cap [n] = I$ and $W_J \cap [n] = J$. As $W_I \subseteq W_J$, we have $W_I \cap [n] \subseteq W_J \cap [n]$. Hence $I \subseteq J$.

Now assume that $I \subseteq J$. Again, as min-cuts, $W_I \cap [n] = I$ and $W_J \cap [n] = J$, and therefore $(W_I \cap W_J) \cap [n] = I$ and $(W_I \cup W_J) \cap [n] = J$. This means $W_I \cap W_J$ and $W_I \cup W_J$ are respectively cuts for I and J . Then submodularity and minimality, applied to $W = W_J$ and $W' = W_I$ as in the proof of (a) above, imply $W_I \cap W_J = W_I$, which proves the claim.

(c) By the definitions, $W_I \cap W_J = \emptyset$ implies that $I \cap J = \emptyset$.

For the converse, suppose that $I \cap J = \emptyset$ and that there exists a vertex $x \in W_I \cap W_J$. Let a, b and c be the total weight of edges from x to, respectively, $W_I \setminus W_J$, $W_J \setminus W_I$ and $[N] \setminus (W_I \cup W_J)$. Since W_I is a min-cut, $a > b + c$, for otherwise we could remove x from W_I without increasing the weight of the cut. Similarly, by considering W_J , we have $b > a + c$. As edge weights are nonnegative, this gives the desired contradiction.

(d) Firstly, we renumber the vertices $n+1, \dots, N$ in K_N so that vertices $[m]$ cover all of the vertices in the union of the W_I . In K_{m+1} we will let $m+1$ take the role of the sink N and adjust weights as follows. We leave the edge weights unchanged between edges with both endpoints in $[m]$. For $i \leq m$ we give edge $(i, m+1)$ the weight corresponding to the sum of the weights of all edges (i, j) with $j = m+1, \dots, N$. It is easy to verify that the weights of the min-cuts W_I are preserved: if a smaller weight cut for a terminal set I existed in K_{m+1} , then it could be reproduced in the original K_N , a contradiction. \square

Unfortunately, part (b) above does not generalize to the intersection of three or more sets. A simple example is given by the K_5 star graph with unit weights for the 3 terminal edges and zero for the sink edge. In particular, the intersection of the three pairs of terminals is of course empty, but the intersection of their minimal min-cuts is not as it contains the bulk vertex.

Each S -vector is realized in K_N for some N , and we are interested in the smallest such N . More generally, for a given n , is there a smallest integer $m(n)$ such that all S -vectors on $[n]$ can be realized in $K_{m(n)}$? The answer is yes and this was proved by Bao et al. [1] (Lemma 6) who obtained $m(n) \leq 2^{2^n - 1}$. A tighter bound can be obtained from Theorem 1 as follows.

Let $Bool_n$ denote the *Boolean lattice* of all subsets of $[n]$ ordered under inclusion. A family of subsets of $[n]$, $\mathcal{I} \subseteq Bool_n$, is an *upper set* if for each $I \in \mathcal{I}$ and $J \subseteq [n]$ that contains I we have $J \in \mathcal{I}$. For $\mathcal{J} \subseteq Bool_n$, we call \mathcal{J} *pairwise intersecting* if each pair of its constituent subsets has a non-empty intersection. If \mathcal{J} is the empty set or consists of a singleton, we consider \mathcal{J} to be pairwise intersecting. An *antichain* $\mathcal{A} \subseteq Bool_n$ is a collection of subsets of $[n]$ which are pairwise incomparable, i.e. none of them is contained in any of the others. Notice that the minimal elements of any upper set form an antichain \mathcal{A} and that \mathcal{A} is pairwise intersecting if and only if its upper set is. Let $M(n)$ denote the number of pairwise intersecting antichains \mathcal{A} in $Bool_n$. We can use this value to bound $m(n)$ as follows:

Corollary 1. *For $n \geq 2$, every S -vector for n terminals can be realized in $K_{m(n)}$, where*

$$m(n) \leq M(n). \quad (2.10)$$

Proof. We first sketch the argument in [1] for their upper bound on $m(n)$. Suppose a given S -vector on n terminals can be realized in a weighted K_N , for some given N . For $I \subseteq [n]$, W_I partitions the vertex set $[N]$ of K_N into two subsets. If we intersect these by W_J , for some $I \neq J \subseteq [n]$, we get 4 subsets, some possibly empty. After repeating for all $2^n - 1$ non-empty

subsets of $[n]$ we obtain a partition of $[N]$ into 2^{2^n-1} subsets, many of which may be empty. However, in each of the non-empty subsets, the vertices of K_N may be merged into a single vertex by combining edge weights (cf. Theorem 1(d)). This new complete graph has at most 2^{2^n-1} vertices and realizes the same min-cut weights as before, giving their result.

To improve this bound we use Theorem 1. For a set $W \subseteq [N]$, denote its complement by $W^c = [N] \setminus W$. Any atom in the partition just described is formed by splitting the non-empty subsets of $[n]$ into two disjoint, spanning families \mathcal{I} and \mathcal{J} , and taking the intersection

$$\bigcap_{I \in \mathcal{I}} W_I \cap \bigcap_{J \in \mathcal{J}} W_J^c. \quad (2.11)$$

Suppose this intersection is non-empty. Theorem 1(c) implies that \mathcal{I} is pairwise intersecting, for otherwise the left intersection in (2.11) is empty. In particular, this implies that both a subset and its complement cannot be in \mathcal{I} . In addition, one can show that \mathcal{I} must either be empty or an upper set in $Bool_n$ as follows. If $\mathcal{I} = \emptyset$, then (2.11) is in fact never empty because it will always contain vertex N . As for $\mathcal{I} \neq \emptyset$, consider two subsets $I \subset K \subseteq [n]$ and suppose $I \in \mathcal{I}$ is non-empty. We have by Theorem 1(b) that $W_I \subseteq W_K$ and so $W_I \cap W_K^c = \emptyset$, implying that if $K \in \mathcal{J}$, then (2.11) is empty. As a result, either $\mathcal{I} = \emptyset$ or \mathcal{I} must be a pairwise intersecting upper set in $Bool_n$, with \mathcal{J} containing all other non-empty subsets of $[n]$.

Because empty atoms from (2.11) do not contribute to min-cut weights, it follows that when considering S -vectors we need only be concerned with pairwise intersecting upper sets \mathcal{I} in $Bool_n$ and $\mathcal{I} = \emptyset$. As described above, the upper sets can be equivalently enumerated as the number of pairwise intersecting antichains in $Bool_n$. Since $M(n)$ counts their number, we conclude that all S -vectors with n terminals can be realized in $K_{M(n)}$. \square

We have the following reasonably tight asymptotic bounds on $M(n)$. Let $\bar{M}(n)$ be the total number of antichains in $Bool_n$. Then,

$$\binom{n}{\lfloor \frac{n}{2} \rfloor + 1} < \log_2 M(n) < \log_2 \bar{M}(n) \sim \binom{n}{\lfloor \frac{n}{2} \rfloor} \sim \frac{2^{n+1}}{\sqrt{2\pi n}}. \quad (2.12)$$

The asymptotic upper bound on $\bar{M}(n)$ is due to Kleitman and Markowsky [19]. The lower bound can be obtained by considering all subsets of $[n]$ of size $\lfloor n/2 \rfloor + 1$. Each pair of such subsets intersects and none can properly contain another. So any collection of these subsets forms an intersecting antichain. While we do not know of tighter asymptotic bounds for $M(n)$, exact values are known [4]³ for $1 \leq n \leq 8$:

$$2, 4, 12, 81, 2646, 1422564, 229809982112, 423295099074735261880. \quad (2.13)$$

However, it seems that $M(n)$ is a very poor upper bound on $m(n)$. For example, data for $1 \leq n \leq 4$ shows that $m(n) = 2, 3, 5, 6$ – see Section 5 for more details.

Problem 1. Find tighter bounds on $m(n)$. In particular, does $\log_2 m(n)$ admit an upper bound that is polynomial in n ?

Definition 1 suggests the following family of cones, which are useful in proving the polyhedrality of H_n . For any pair of integers n and N such that $2 \leq n+1 \leq N$, consider

$$H_{N,n} = \text{conv} \{S \in \mathbb{R}^{2^n-1} : \text{nonnegative weighted } K_N \text{ s.t. } S \text{ satisfies (2.2)}\}. \quad (2.14)$$

This is a generalization of the cone defined by the cut functions, which corresponds to the specific case $n = N - 1$. Without the convex hull operator in (2.14), $H_{N,n}$ would not be convex

³ $M(n)$ is entry $n+1$ in Proposition 1.2 of [4].

in general, as shown by example in Appendix C. An important property of $H_{N,n}$ is that it is naturally invariant under the action of the symmetric group Sym_n which permutes the elements of the set $[n]$. In fact, $H_{N,n}$ enjoys a larger symmetry group: it is symmetric under permutations of vertices in the extended terminal set $[n; N]$. The permutations of K_N under Sym_{n+1} yield S -vectors (2.1) which are related by the simple fact that $C(W) = C(W^c)$. Similarly, in an undirected graph any min-cut is insensitive to the exchange of its sources and sinks. When talking about symmetries under Sym_{n+1} , it is thus convenient to identify $S_{[n;N]\setminus I} = S_I$.

It is easy to see that in general $H_{N,n} \subseteq H_{N+1,n}$, since an additional bulk vertex can always be added to K_N with all edges containing it of weight zero. We are now able to prove that H_n is a convex polyhedral cone. Our bound is tighter than the original proof given in [1] due to our use of antichains.

Corollary 2. *For any $n \geq 1$, H_n is a convex, polyhedral cone given by $H_n = H_{m(n),n}$.*

Proof. Firstly, suppose $S \in H_n$. Then for some N and weight set w the pair (S, w) satisfies (2.2) and so $S \in H_{N,n} \subseteq H_n$. Conversely, suppose S is in the convex hull of extreme rays of H_n . Each of these rays can be realized in a weighted K_N for some $N \leq m(n)$. For a specific conical combination of extreme rays giving S , consider the graph obtained by identifying all of their associated graphs at their terminal vertices, each with its edge weights multiplied by the coefficient in the associated conical combination. This graph clearly still realizes S ,⁴ and can be thought of as a K_N for some large but finite N with many zero-weight edges omitted. However, the bound on N in Corollary 1 guarantees that by merging vertices this graph can be reduced to one with $N \leq m(n)$, thus proving convexity. \square

Of course, H_n inherits the Sym_{n+1} symmetry discussed above. As a result, when considering the extremal structure of H_n , we will only specify single representatives of symmetry orbits under Sym_{n+1} .

Almost nothing is known about the complexity of computational problems related to H_n .

Problem 2. Given a vector $q \in \mathbb{Z}^{2^n-1}$, what is the complexity of deciding if $q \in H_n$? What is the complexity of deciding whether $qx \geq 0$ is satisfied for all $x \in H_n$?

2.2 Representations of the HEC

A basic result of polyhedral geometry is that any polyhedral cone C can be represented by a non-redundant set of facet-defining inequalities, which we can write as $Ax \geq 0$ for a suitably dimensioned matrix A and variables x , and is called an H -representation. One can also represent C by a non-redundant list E of its extreme rays, such that $C = \text{conv}\{E\}$, which is called a V -representation. Both representations are unique up to row scaling. In this paper we are concerned with computing the H - and V -representations of H_n . Normally, for cones (or polyhedra) arising in discrete optimization, we have available one or the other of the representations. However, this is not the case for H_n . To proceed we will initially try to find both *valid inequalities* for C , which are those satisfied by all rays in C , and to find *feasible rays* of C . A set of valid inequalities forms an *outer approximation* of H_n and a set of valid rays forms an *inner approximation*. The following well known basic result shows when such sets respectively constitute an H - and V -representation (see, e.g., Schrijver [25]).

⁴This is basically the statement that any flow network problem with multiple source/sink vertices can be equivalently reformulated in terms of a single supersource/supersink vertex connected to each of the sources/sinks with edges of infinite capacity. In our case, however, it is preferable to simply merge together terminals of the same type into a single “superterminal”, rather than having unnecessary infinite-weight edges.

Proposition 2. For a given polyhedral cone C , let $Ax \geq 0$ be a non-redundant set of valid inequalities and let E be a non-redundant set of feasible rays. Then:

- (a) An extreme ray of $Ax \geq 0$ is an extreme ray of C if it is feasible for C .
- (b) A facet of $\text{conv}\{E\}$ is a facet of C if it is valid for C .
- (c) E is precisely the set of extreme rays of $Ax \geq 0$ if and only if they respectively constitute V - and H -representations of C .

Parts (a) and (b) lead to a kind of bootstrapping process which terminates once (c) can be applied. This is described in detail in Section 6, but to illustrate we now look at some small values of n .

For $n = 1$, the S -vectors are the nonnegative real numbers. There is one facet $S_1 \geq 0$ and one extreme ray with $S_1 = 1$, and Proposition 2(c) is readily verified. Notice that this simple $n = 1$ extreme ray can be represented in K_2 with the single edge $(1, 2)$ having weight 1. More generally, any K_N where two distinct singletons $i, j \in [n; N]$ share a unit-weight edge and all other weights are zero will be called an (i, j) Bell pair. The S -vector of such a Bell pair has nonzero $S_I = 1$ if and only if either $i \in I$ or $j \in I$, but not both.

For $n = 2$ we have $S = (S_1, S_2, S_{12})$ and a valid inequality $S_1 + S_2 \geq S_{12}$. This follows since the union of cuts for two terminals $i, j \in [n; N]$ is always a cut for the union of the two terminals $\{i, j\}$. Hence the latter's min-cut cannot have larger weight than the sum of the weights of the two other cuts. The full orbit of $S_1 + S_2 \geq S_{12}$ contains $S_1 + S_{12} \geq S_2$ and $S_{12} + S_2 \geq S_1$. All three are related by the S_3 symmetry of permutations of $[2; N]$ and the identification of $S_{[2; N] \setminus I} = S_I$ for all $I \subseteq [2; N]$. In the context of information theory, the first one is known as *subadditivity* (SA), while the latter two are called the Araki-Lieb inequalities.

Subadditivity generalizes to a valid inequality for any disjoint, non-empty subsets of terminals I, J with $I \cup J \subseteq [n; N]$ to give

$$\text{SA:} \quad S_I + S_J \geq S_{I \cup J}. \quad (2.15)$$

We exclude $I \cup J = [n; N]$ since in this case SA reduces to nonnegativity. Every inequality in the enlarged symmetry orbit Sym_{n+1} of (2.15) clearly remains valid. For any disjoint subsets of terminals $I, J \subseteq [n; N]$, those of Araki-Lieb type take the form $S_I + S_{I \cup J} \geq S_J$. The qualitative difference between SA and Araki-Lieb is that in the former the disjoint subsets $I, J \subseteq [n; N]$ do not contain the sink, whereas in the latter one of them does, and whenever $N \in I \subseteq [n; N]$ one identifies $S_I = S_{[n; N] \setminus I}$. For future convenience, we introduce

$$q_{I:J}S = S_I + S_J - S_{I \cup J}, \quad (2.16)$$

known as the *mutual information* in the physics community. This way, SA corresponds to the nonnegativity of the mutual information $q_{I:J}S \geq 0$.

Proceeding as suggested by Proposition 2(a), we can compute the extreme rays arising from (2.15) by the action of Sym_3 , together with the 3 nonnegativity inequalities (in fact, the latter are redundant and can be ignored). Doing so we obtain 3 extreme rays related by symmetry, of which one is $S = (1, 1, 0)$. This can be represented in K_3 by a $(1, 2)$ Bell pair. Obviously, this can also be obtained from the $(1, 2)$ Bell pair for $n = 1$ in K_2 by adding a new vertex with all edge weights to it zero. This is a process called a *zero-lifting* of extreme rays and which we discuss in detail in Section 3.2. So if we let E be the set of 3 output rays and $Ax \geq 0$ be the 3 SA inequalities we are again done by Proposition 2(c).

3 Extreme rays

Since we do not have an H -representation of $H_{N,n}$ we have no direct way to compute its extreme rays. In this section we introduce a lifting of $H_{N,n}$ to a cone for which we can explicitly write an H -representation. Computing the extreme rays of this cone and then making a projection allows us to compute a superset of the extreme rays of $H_{N,n}$. This construct provides the first systematic procedure for obtaining H_n , thus significantly improving on the random searches used so far in building the HEC [1, 14]. We also describe a zero-lifting operation, which allows known extreme rays for S -vectors defined on n terminals to generate extreme rays for those defined on $n + 1$ terminals.

3.1 A lifting of the HEC

For integers n and N such that $3 \leq n + 1 \leq N$, consider the following system of inequalities whose variables are the S -vector entries S_I and the edge weights $w(e)$ of K_N :

$$S_I \leq \|C(W)\|, \quad \forall W \subseteq [N - 1], \emptyset \neq I \subseteq [n] \text{ s.t. } I = W \cap [n], \quad (3.1a)$$

$$w(e) \geq 0, \quad \forall e \in E_N. \quad (3.1b)$$

Note that for each cut $C(W)$ there is precisely one I such that $I = W \cap [n]$. Since we are excluding the case $I = \emptyset$, this implies that (3.1a) contains $2^{N-1} - 2^{N-n-1}$ inequalities. There are an additional $N(N - 1)/2$ nonnegative inequalities from (3.1b). Since each $\|C(W)\|$ is just a sum of weights $w(e)$ for every $e \in C(W)$, together with the $2^n - 1$ variables S_I , there are a total of $M_{N,n} = 2^n - 1 + N(N - 1)/2$ variables involved in (3.1). Let (S, w) denote a vector of length $M_{N,n}$ representing these variables.

Definition 2. The cone $P_{N,n}$ denotes the set of all (S, w) satisfying (3.1).

Since $P_{N,n}$ is given explicitly by (3.1), it is a rational cone. Note that the variables S_I in $P_{N,n}$ are not bounded from below. One could add the inequalities $S_I \geq 0$ but this greatly increases the complexity of the cone, as explained below.

The cones $H_{N,n}$ and $P_{N,n}$ cannot be directly compared, since they are defined in different dimensional spaces. So we first define a lifting of $H_{N,n}$ by

$$H_{N,n}^+ = \text{conv} \{(S, w) \in P_{N,n} : S \in H_{N,n}\}. \quad (3.2)$$

which is by definition a subset of $P_{N,n}$ and whose projection onto the S coordinates is $H_{N,n}$. We similarly define H_n^+ . An example in Appendix C shows that $H_{N,n}^+$ is in general non-convex without the convex hull operator. It is easy to see that $P_{N,n}$ contains $M_{N,n}$ *trivial* extreme rays. These are formed by setting either one $S_I = -1$ or one $w(e) = 1$, and all other variables zero.

Each extreme ray of $H_{N,n}$ is the projection of a non-trivial extreme ray of $P_{N,n}$, as we now show:

Theorem 2.

- (a) If (S, w) is a non-trivial extreme ray of $P_{N,n}$, then $S \in H_{N,n}$.
- (b) If S is an extreme ray of $H_{N,n}$, then there is a weight vector w such that (S, w) is a non-trivial extreme ray of $P_{N,n}$.

Proof.

- (a) Suppose that (S, w) defines a non-trivial extreme ray of $P_{N,n}$. Then there must be a set of at least $M_{N,n} - 1$ inequalities in (3.1) satisfied as equations whose solutions have the form $\lambda(S, w)$, with $\lambda \geq 0$. Each S_I must be present in at least one of these equations or else it could be increased independently of the others and the resulting vector (S', w) would still be a solution of the equations but not of that form. This in turn implies that S satisfies (2.2) for the given weight function w . Hence $S \in H_{N,n}$.
- (b) Suppose S is an extreme ray of $H_{N,n}$. Since S satisfies (2.2), all of its values are non-negative and there must exist a corresponding weight assignment \bar{w} . We now define a face F of $P_{N,n}$ by intersecting it with the hyperplanes

$$S_I = \|C(W)\|, \quad \forall W \text{ achieving the minimum in (2.2)}, \quad (3.3a)$$

$$w(e) = 0, \quad \forall e \in E_N \text{ s.t. } \bar{w}(e) = 0. \quad (3.3b)$$

Each S_I appears in at least one equation. F is defined by a set of extreme rays of $P_{N,n}$ but none of these can be a trivial ray of the type $S_I = -1$ since $S_I = \|C(W)\| \geq 0$. There may be a trivial extreme ray of the type $w(e) = 1$ as long as $\bar{w}(e) \neq 0$ and the edge e does not appear in any of the cuts $C(W)$ in the system of hyperplanes. Suppose that there are s of these and write each of them as 1_e . Also, denote the non-trivial extreme rays of $P_{N,n}$ that lie on F by (S^i, w^i) , with $i \in [t]$. From part (a) above, we have that $S^i \in H_{N,n}$ for all $i \in [t]$. Writing (S, w) as a conical combination of the extreme rays that define F ,

$$(S, w) = \sum_{i=1}^t \lambda_i (S^i, w^i) + \sum_{j=1}^s \mu_j 1_{e_j}, \quad \lambda_i, \mu_j \geq 0, \quad (3.4)$$

we deduce that $S = \sum_{i=1}^t \lambda_i S^i$. Since S is an extreme ray of $H_{N,n}$ it follows that $S = S^i$ for all i for which $\lambda_i > 0$. For each such i , (S, w^i) is a non-trivial extreme ray of $P_{N,n}$. \square

It was initially hoped that non-trivial extreme rays of $P_{N,n}$ would project to extreme rays of $H_{N,n}$, but an example in Appendix C show that this is not the case. Also, a direct projection of $P_{N,n}$ onto its S coordinates does not give $H_{N,n}$. For any given values of the S coordinates, a feasible solution to inequalities (3.1) can be obtained by choosing any suitably large w coordinates. Hence the projection is simply the whole space R^{2^n-1} . Nevertheless, we do obtain a method in principle for obtaining a complete description of H_n :

Corollary 3. *A V -description of H_n can be obtained by computing the extreme rays (S, w) of $P_{m(n),n}$, projecting to the S coordinates, and removing both the trivial and the redundant rays.*

Proof. By Theorem 2(b) every extreme ray $S \in H_{m(n),n}$ appears in some non-trivial extreme ray (S, w) of $P_{m(n),n}$. Projecting the latter to the S coordinates produces all extreme rays of $H_{m(n),n}$. Redundant rays can be removed by linear programming. Since $H_n = H_{m(n),n}$, the result follows by Corollary 2. \square

This important new result allows for a constructive derivation of H_n (for which no explicit representation is known) starting from $P_{m(n),n}$ (for which a V -representation is straightforward to write down). Since $P_{m(n),n}$ is a rational cone, as remarked earlier, it follows that H_n is also. This fact, proven in Proposition 7 of [1] by a different technique, means extreme rays and facets always admit integral representations. With our current upper bound on $m(n)$ the computation is impractical except for small values of n . It does not help here to include the extra inequalities $S_I \geq 0$ because this introduces a large number of new extreme rays (S, w) of $P_{N,n}$ which are

not valid pairs. For example, while $P_{6,4}$ has 50 extreme rays of which 15 are trivial, adding nonnegativity yields 49915 extreme rays, all but 35 of which do not yield valid (S, w) pairs. A computationally lighter method to test whether a given S -vector is realizable is as follows:

Theorem 3. *If $\bar{S} \in H_{N,n}$, then there is a weight vector \bar{w} such that (\bar{S}, \bar{w}) is a vertex of the polyhedron Q defined as the intersection of $P_{N,n}$ and the hyperplanes $S = \bar{S}$.⁵*

Proof. First we suppose that $\bar{S} \in H_{N,n}$. Then there exists a weight vector \bar{w} for K_N that realizes \bar{S} . By construction (\bar{S}, \bar{w}) is contained in Q and so Q is non-empty. Since all components of S in Q are fixed, Q is a possibly unbounded polyhedron with vertices of the form (\bar{S}, w) and possibly additional extreme rays of the form 1_{e_j} for edges e_j that do not appear in any minimum-weight cut W obeying $W \cap [n] = I$ and $\|C(W)\| = S_I$. We can write

$$(\bar{S}, \bar{w}) = \sum_{i=1}^t \lambda_i (\bar{S}, w^i), \quad \sum_{i=1}^t \lambda_i = 1, \quad \lambda_i \geq 0, \quad (3.5)$$

for a set of t vertices (\bar{S}, w^i) of Q . For a cut W in K_N , let $\|\bar{C}(W)\|$ and $\|C^i(W)\|$ denote its weight using \bar{w} and w^i , respectively. Since \bar{w} is a realization of \bar{S} , for each $\emptyset \neq I \subseteq [n]$ there exists a min-cut W_I such that $\bar{S}_I = \bar{C}(W_I)$. Now, by (3.5) and the linearity of the cut weight function,

$$\|\bar{C}(W_I)\| = \sum_{i=1}^t \lambda_i \|C^i(W_I)\|, \quad \sum_{i=1}^t \lambda_i = 1, \quad \lambda_i \geq 0. \quad (3.6)$$

Hence by (3.1a) we must also have $\bar{S}_I = \|C^i(W_I)\|$ for all $i \in [t]$. It follows that each (\bar{S}, w^i) is a vertex of Q representing \bar{S} . \square

We now show how these theorems can help in determining the extremal structure of H_3 . For example, we can compute the extreme rays of $P_{5,3}$, project onto the S -coordinates, delete the trivial rays and remove redundancy, getting a V -representation of $H_{5,3}$. It contains 17 extreme rays in 7 dimensions. The H -representation of $H_{5,3}$ is easy to compute and contains 7 facets. One facet is new and the other 6 are SA inequalities:

$$S_i + S_j \geq S_{ij}, \quad i \neq j \in [3; N], \quad (3.7)$$

where N is the sink and we recall that $S_{[3;N] \setminus I} = S_I$. Earlier we saw that for $n = 2$ there is one SA orbit of 3 facets: $S_1 + S_2 \geq S_{12}$, $S_1 + S_{12} \geq S_2$, and $S_{12} + S_2 \geq S_1$. Although the first one remains a facet of the form of (3.7) for $n = 3$, the other two do not, which may seem surprising. We return to this in Section 4.2 when discussing the lifting of facets (see Proposition 8).

The cone $H_{5,3}$ has one new facet which is inequality (4.2) below. If we can prove this is valid for H_3 then, by Proposition 2(c), we will have complete H - and V -representations. How to prove validity of an inequality is discussed in Section 4.

3.2 Zero-lifting extreme rays

Extreme rays for $P_{N,n}$ remain extremal for larger values of N as the following result describes:

Proposition 3. *If (S, w) is an extreme ray of $P_{N,n}$, then, by adding suitably many new weight coordinates set to zero, it is an extreme ray (S, w') of $P_{N',n}$ for every $N' > N$. Hence $P_{N,n}$ is a projection of $P_{N',n}$.*

⁵The converse of this is false, as Q generally has many vertices (\bar{S}, w) for which w does not realize \bar{S} .

Proof. Let (S, w) define an extreme ray of $P_{N,n}$ and consider the base graph K_{N+1} . We extend the weight vector w by adding N new coordinates to get a vector w' of length $(N+1)N/2$. We set $w'(i, j) = w(i, j)$ for $1 \leq i < j < N$ and $w'(i, N+1) = w(i, N)$ for $1 \leq i < N$. All edges containing vertex N receive weight zero in w' , and vertex $N+1$ is the new sink. Since N is now a bulk vertex, it may participate in a cut W , but since $\|C(W)\| = \|C(W \cup \{N\})\|$, it will never change its total weight. Hence $(S, w') \in P_{N+1,n}$. Since (S, w) defines an extreme ray of $P_{N,n}$ we can choose $M_{N,n} - 1$ inequalities in (3.1) which, when satisfied as equations, have solutions in $P_{N,n}$ of the form $\lambda(S, w)$ with $\lambda \geq 0$. To these equations we add the N equations $w(i, N) = 0$. The resulting system has solutions in $P_{N+1,n}$ of the form $\lambda(S, w')$ with $\lambda \geq 0$, and the extremality of the ray defined by (S, w') follows. \square

Extreme rays can also be preserved under the addition of new terminal vertices as follows. Given $(S, w) \in P_{N,n}$, we define its *zero-lift* as the vector $(S', w') \in P_{N+1,n+1}$, where S' has dimension $2^{n+1} - 1$ and w' has dimension $(N+1)N/2$, by

$$S'_{\{n+1\}} = 0, \quad S'_{I \cup \{n+1\}} = S'_I = S_I, \quad \emptyset \neq I \subseteq [n], \quad (3.8a)$$

$$w'(i, n+1) = 0, \quad i \in [n], \quad w'(i, j) = w(i, j), \quad 1 \leq i < j \leq N. \quad (3.8b)$$

Similarly, $S' \in H_{N+1,n+1}$ above defines the *zero-lift* of the given $S \in H_{N,n}$. A vector x that satisfies an inequality $qx \geq 0$ as an equation is called a *root* of that inequality.

Proposition 4. *If (S, w) is an extreme ray of $P_{N,n}$, then its zero-lift (S', w') is an extreme ray of $P_{N+1,n+1}$.*

Proof. Let (S, w) define an extreme ray of $P_{N,n}$. For each $\emptyset \neq I \subseteq [n]$ choose an inequality from (3.1a) for which it is a root. These are linearly independent inequalities since the S_I coordinates define minus the identity matrix. To these inequalities add all those from (3.1b) for which (S, w) is a root. Since (S, w) is an extreme ray we have a linearly independent set of $2^n + N(N-1)/2 - 2$ such inequalities. Call this system L . We now add terminal $n+1$ and define S' and w' as above. It is easy to verify that $(S', w') \in P_{N+1,n+1}$. Note $P_{N+1,n+1}$ has $2^n + N$ more dimensions than $P_{N,n}$ and we will augment L by this many linearly independent inequalities. Firstly, for each $\emptyset \neq I \subseteq [n]$ the inequality previously chosen will also be satisfied as an equation when I is replaced by $I \cup \{n+1\}$. This gives an additional $2^n - 1$ inequalities which are linearly independent from the others in L since the new variables $S_{I \cup \{n+1\}}$ again form minus the identity matrix. To these we add N equations $w(i, n+1) = 0$ for $1 \leq i \leq n$ and the equation $S_{\{n+1\}} = \|C(\{n+1\})\|$. This gives L the required number of tight linearly independent constraints. By construction, their solution is $\lambda(S', w')$ with $\lambda \geq 0$, which proves that (S', w') defines an extreme ray of $P_{N+1,n+1}$. \square

The following result, though not unexpected, is proved here for the first time:

Proposition 5. *If S is an extreme ray of H_n , then its zero-lift S' is an extreme ray of H_{n+1} . Hence H_n is a projection of H_{n+1} .*

Proof. If S is an extreme ray of H_n , then it is a root of a linearly independent set of $2^n - 2$ of its facet inequalities. Clearly S' is also a root of these inequalities. Additionally, S' is a root of the following $2^n - 1$ instances of SA,

$$S'_I + S'_{\{n+1\}} \geq S'_{I \cup \{n+1\}}, \quad (3.9)$$

for all $\emptyset \neq I \subseteq [n]$, and also obeys $S'_{\{n+1\}} = 0$. This gives 2^n more equations which are linearly independent and are also independent of the former $2^n - 2$ because they independently involve the new, distinct variables $S'_{I \cup \{n+1\}}$ for every $I \subseteq [n]$. Since S' satisfies $2^{n+1} - 2$ independent valid inequalities as equations, it is an extreme ray of H_{n+1} by Proposition 2(a). \square

To illustrate the use of the results in this subsection we consider the case $n = 4$. If we compute $P_{6,4}$ and remove the trivial rays we have 35 extreme rays. When we project onto the 15 coordinates S_I and remove redundancy, there remain 20 extreme rays. Only 5 of these are new, whereas the other 15 come from zero-lifts of the two extreme-ray classes that define H_3 . The convex hull of this set is bounded by 20 facets that are examples of what is called zero-lifting from the two facet classes for H_3 . We will define this process and prove that it preserves validity and facets in Section 4.2. By this result and Proposition 2(c) we have obtained the H - and V -representations of H_4 .

4 Valid inequalities and facets

As remarked in Section 2, there is no general explicit H -representation known for H_n , although it can in principle be computed by using the method of Corollary 3 and then converting the resulting V -representation into an H -representation. In Section 5 we give an integer linear program (ILP) for testing whether an inequality is valid over H_n or not. However, to prove validity would require solving an ILP whose size depends on $m(n)$ and so is impractical with current bounds. The main result of this section is a tractable method known as *proof by contraction* to prove inequalities valid for H_n . By exhibiting the required number of extreme rays it is then possible to prove they are facets.

A general inequality $qS \geq 0$ over H_n is specified by a vector $q \in \mathbb{R}^{2^n-1}$. Let $K \subseteq [n]$ be the subset of terminals appearing in it, i.e. $i \in K$ if and only if $q_I \neq 0$ for some $I \ni i$. If $|K| < n$, one can turn it into an inequality over $H_{|K|}$ by relabelling terminals $K \rightarrow [|K|]$, if necessary. We say that an inequality over H_n is in *canonical form* if $|K| = n$, and write it canonically as

$$\sum_{l=1}^L \alpha_l S_{I_l} \geq \sum_{r=1}^R \beta_r S_{J_r}, \quad (4.1)$$

where L and R are respectively the number of positive and negative entries in the vector q , and for all $l \in [L]$ and $r \in [R]$, the coefficients $\alpha_l, \beta_r > 0$ and the sets $I_l, J_r \subseteq [n]$ are distinct and non-empty. Because H_n is a rational cone, the normalization of (4.1) of any inequality of interest is always set such that all coefficients $\alpha_l, \beta_r > 0$ are together coprime integers.

At the end of Section 2.2 we discussed the cases $n = 1, 2$. Recall that H_1 is 1-dimensional and corresponds to a nonnegative half-line. Its only facet is $S_1 \geq 0$, which trivially follows from nonnegativity of the weights in (2.14). For $n = 2$, we saw that the resulting 3-dimensional cone H_2 is a simplex bounded by the 3 facets in the symmetry orbit of the SA inequality (2.15). We discussed H_3 at the end of Sections 3.1 and 3.2. Apart from the SA orbit, containing 6 facet inequalities, an additional inequality was discovered to bound H_3 [12]:

$$S_{12} + S_{13} + S_{23} \geq S_1 + S_2 + S_3 + S_{123}. \quad (4.2)$$

This is known in physics as the *monogamy of mutual information* (MMI) due to its rewriting using (2.16) as $q_{1:23}S \geq q_{1:2}S + q_{1:3}S$. Since one can write submodularity as $q_{1:23}S \geq q_{1:2}S$, by nonnegativity of $q_{1:3}S \geq 0$ one sees that MMI is a strictly stronger inequality. The proof of the validity of (4.2) will be presented in Section 4.1 (see Table 1) as an example of a general combinatorial proof method for valid inequalities of H_n . This will show that H_3 has 7 facets and so is also a simplex. As we saw at the end of Section 3.2, no new inequalities arise for $n = 4$. However, for $n \geq 3$ note that MMI acquires a more general form which we show is valid for H_n : for disjoint non-empty subsets $I, J, K \subseteq [n]$,

$$\text{MMI:} \quad S_{IJ} + S_{IK} + S_{JK} \geq S_I + S_J + S_K + S_{IJK}, \quad (4.3)$$

which is valid for H_n , as we show in Section 4.2.

4.1 Proof by contraction

We now describe the proof-by-contraction method for proving validity of inequalities for H_n . Although our description is complete, we refer the reader to [1] and [3] for more details on its derivation. By making use of antichains, as in Corollary 1, we obtain a stronger result than previous ones. Our discussion will be exemplified with MMI as given in (4.2).

To set the stage, let $Q_m = \{0, 1\}^m \subset \mathbb{R}^m$ denote the (vertices of) the unit m -cube and refer to $x \in Q_m$ as a *bitstring*. At times, it will also be useful to think of Q_m as an m -ary Boolean domain. Given some vector of positive entries $\gamma \in \mathbb{R}_+^m$, we can turn Q_m into a metric space with distance function d_γ by endowing it with a weighted Hamming norm $\|\cdot\|_\gamma$ via

$$d_\gamma(x, x') = \|x - x'\|_\gamma, \quad \|x\|_\gamma = \sum_{k=1}^m \gamma_k |x_k|. \quad (4.4)$$

Consider now a candidate inequality in canonical form over H_n , written as in (4.1). Encode each side of it into $n + 1$ *occurrence vectors*, $x^{(i)} \in Q_L$ and $y^{(i)} \in Q_R$ for $i \in [n; N]$, with entries

$$x_i^{(i)} = \delta(i \in I_l), \quad y_r^{(i)} = \delta(i \in J_r), \quad (4.5)$$

where δ is a Boolean indicator function, i.e. it yields 1 or 0 depending on whether its argument is true or false, respectively. Clearly, the occurrence vectors for $i = N \notin [n]$ are all-0 vectors. For inequality (4.2), the $i \in [n]$ occurrence vectors are the following bitstrings:

$$\begin{aligned} x^{(1)} &= (1, 1, 0), & y^{(1)} &= (1, 0, 0, 1), \\ x^{(2)} &= (1, 0, 1), & y^{(2)} &= (0, 1, 0, 1), \\ x^{(3)} &= (0, 1, 1), & y^{(3)} &= (0, 0, 1, 1). \end{aligned} \quad (4.6)$$

Bitstrings are a bookkeeping device for partitioning the vertex set $[N]$ of K_N into specific disjoint subsets suitable for studying a given candidate inequality. In particular, consider the minimal min-cuts W_{I_l} for $l \in [L]$ associated to every term on the left-hand side of (4.1). Each of the 2^L different bitstrings $x \in Q_L$ indexes a disjoint vertex subset $W(x) \subseteq [N]$ defined by

$$W(x) = \bigcap_{l=1}^L W_{I_l}^{x_l}, \quad W^b = \begin{cases} W & \text{if } b = 1, \\ W^c & \text{if } b = 0. \end{cases} \quad (4.7)$$

The attentive reader will notice that these $W(x)$ sets would be precisely the atoms introduced in (2.11) when proving Corollary 1 if one were to iterate the intersection over all possible $2^n - 1$ non-empty subsets of $[n]$. In the current discussion, one need only consider the pertinent L subsets $I_l \subseteq [n]$ involved in the left-hand side of (4.1). The resulting $W(x)$ sets are again disjoint by construction, i.e. $W(x) \cap W(x') = \emptyset$ unless $x = x'$. The converse is certainly not true though, as expected from Corollary 1. In particular, $W(x)$ will be empty whenever the family of sets $\mathcal{I}(x) = \{I_l \subseteq [n] : x_l = 1\}$ is not a pairwise intersecting upper set in $\mathcal{I}_L = \{I_l \subseteq [n] : l \in [L]\}$. The relation between this statement and the one in Corollary 1 that refers to upper sets in $Bool_n$ is better understood in terms of their associated antichains. Namely, $W(x)$ will be empty whenever the minimal elements in $\mathcal{I}(x)$ are not a pairwise intersecting antichain in \mathcal{I}_L , which holds if and only if the same is true in $Bool_n$. In other words, there is a non-trivial $W(x)$ precisely for every pairwise intersecting antichain in $Bool_n$ that is also so in \mathcal{I}_L , and thus the number of relevant bitstrings will be considerably smaller than $M(n)$.

The discussion above motivates introducing the subset $A_n(\mathcal{I}_L) \subseteq Q_{2^n - 1}$ of all bitstrings $x \in A_n(\mathcal{I}_L)$ such that $\mathcal{I}(x)$ is a pairwise intersecting antichain in \mathcal{I}_L . Crucially, these suffice

to characterize the minimal min-cuts for $I_L \in \mathcal{I}_L$ in any K_N , in the sense that these are all reconstructible via

$$W_{I_L} = \bigcup_{x: x_l=1} W(x), \quad (4.8)$$

where the union here, and in all that follows next, runs over all bitstrings $x \in A_n(\mathcal{I}_L)$ subject to the given conditions. Furthermore, one can use these vertex sets $W(x)$ to construct (not necessarily minimum) cuts for any subset of terminals $J \subseteq \bigcup_{l=1}^L I_l \subseteq [n]$. To see this, let $i \in [n]$ be any one of the terminals involved in the subsets $I_l \in \mathcal{I}_L$. We want to find which of the $W(x)$ sets the vertex i lands on. Since $i \in W_{I_l}$ if and only if $i \in I_l$ by the definition of a cut for I_l , it follows that $i \in W(x)$ if and only if $x_l = 1$ precisely when $I_l \ni i$ and $x_l = 0$ otherwise. In other words, the bitstring we are after is precisely the occurrence vector $x^{(i)} \in Q_L$ defined in (4.5), and we thus have $i \in W(x^{(i)})$.

Lemma 1. *Let $f : Q_m \rightarrow \{0,1\}$ be an m -ary Boolean function. Given some collection of terminal subsets $\mathcal{I}_L \ni I_l$ and the partitioning of $[N]$ defined in (4.7), construct the vertex set*

$$U^f = \bigcup_{x: f(x)=1} W(x). \quad (4.9)$$

Then, for any subset of terminals $J \subseteq \bigcup_{l=1}^L I_l \subseteq [n]$, we have

$$U^f \cap [n] = J \quad \iff \quad f(x^{(i)}) = \delta(i \in J), \quad \forall i \in [n]. \quad (4.10)$$

Proof. A trivial rephrasing of $U^f \cap [n] = J$ is that, for $i \in [n]$, one has $i \in J$ if and only if $i \in U^f$. Since $i \in W(x^{(i)})$ for every $i \in [n]$ and all $W(x)$ are disjoint, it follows that $i \in U^f$ if and only if $W(x^{(i)}) \subseteq U^f$. Finally, since by construction $W(x^{(i)}) \subseteq U^f$ if and only if $f(x^{(i)}) = 1$, the desired result is obtained. \square

The min-cut edges $C(W_{I_l})$ can also be conveniently organized in terms of bitstrings via

$$E(x, x') = \{(i, j) \in E_N : i \in W(x) \text{ and } j \in W(x')\}. \quad (4.11)$$

Because the $W(x)$ vertex sets are disjoint, so are the $E(x, x')$ edge sets for any distinct pair of bitstrings $x, x' \in Q_L$. This leads to the following useful result for $C(W_{I_l})$:

Lemma 2. *The edges of a min-cut W_{I_l} for some $I_l \in \mathcal{I}_L$ and their total weight are, respectively,*

$$C(W_{I_l}) = \bigcup_{x, x': x_l \neq x'_l} E(x, x'), \quad \|C(W_{I_l})\| = \sum_{x, x'} |x_l - x'_l| |E(x, x')|, \quad (4.12)$$

where the index sets are unordered pairs of bitstrings $x, x' \in A_n(\mathcal{I}_L)$.

Proof. By definition, an edge $(i, j) \in C(W_{I_l})$ if and only if $i \in W_{I_l}$ and $j \in W_{I_l}^c$. Using (4.8), one can write $W_{I_l} = \bigcup_{x: x_l=1} W(x)$ and, similarly, $W_{I_l}^c = \bigcup_{x: x_l=0} W(x)$. Hence $(i, j) \in E(x, x')$ is contained in $C(W_{I_l})$ if and only if x and x' differ in their l^{th} bit $x_l \neq x'_l$. It follows that $C(W_{I_l})$ can be constructed by joining all edge sets $E(x, x')$ with bitstrings $x, x' \in A_n(\mathcal{I}_L)$ such that $x_l \neq x'_l$, thereby proving the first equation in (4.12). Furthermore, since all $E(x, x')$ are disjoint for distinct pairs of bitstrings, the total weight of their union reduces to the sum over the total weights of every $E(x, x')$ involved, which is precisely what the second equation computes. \square

Given two metric spaces (M, d) and (M', d') , we call $f : M \rightarrow M'$ a d - d' contraction map if

$$d'(f(x), f(y)) \leq d(x, y), \quad \forall x, y \in M. \quad (4.13)$$

The general proof method can now be stated:

Theorem 4. Inequality (4.1) is valid for H_n if there exists a d_α - d_β contraction map

$$f : A_n(\mathcal{I}_L) \rightarrow Q_R, \quad (4.14)$$

satisfying $f(x^{(i)}) = y^{(i)}$ for all $i \in [n; N]$.

Proof. Associate a cut U_{J_r} to each subsystem J_r that appears on the right-hand side of (4.1) by using the map f to pick which sets $W(x)$ to include in the definition of U_{J_r} as follows:

$$U_{J_r} = \bigcup_{x:f(x)_r=1} W(x). \quad (4.15)$$

That this indeed obeys the cut condition $U_{J_r} \cap [n] = J_r$ is guaranteed by Lemma 1 and the fact that f is required to respect occurrence vectors, i.e. $f(x^{(i)}) = y^{(i)}$ for every $i \in [n; N]$.

$$\sum_{l=1}^L \alpha_l S_{I_l} = \sum_{l=1}^L \alpha_l \|C(W_{I_l})\| = \sum_{x,x'} |E(x,x')| \sum_{l=1}^L \alpha_l |x_l - x'_l| = \sum_{x,x'} |E(x,x')| d_\alpha(x,x'). \quad (4.16)$$

Similarly, for the U_{J_r} cuts one has

$$\sum_{r=1}^R \beta_r \|C(U_{J_r})\| = \sum_{x,x'} |E(x,x')| d_\beta(f(x), f(x')). \quad (4.17)$$

Therefore, by hypothesis, the contraction property of f implies

$$\sum_{l=1}^L \alpha_l \|C(W_{I_l})\| \geq \sum_{r=1}^R \beta_r \|C(U_{J_r})\|. \quad (4.18)$$

Because every set U_{J_r} is a cut for each J_r appearing on the right-hand side of (4.1), by minimality $\|C(U_{J_r})\| \geq S(J_r)$ for every $r \in [R]$. Hence the right-hand side of (4.18) is no smaller than that of (4.1). Finally, since their respective left-hand sides are equal, validity of (4.1) follows. \square

This theorem was proved in [1] (Theorem 8) in a somewhat weaker form. Whereas the domain of their contraction map is Q_L , enumerating all subsets of $\mathcal{I}_L \subseteq \text{Bool}_n$, we reduce this to $A_n(\mathcal{I}_L) \subseteq Q_L$, enumerating only the pairwise intersecting antichains in \mathcal{I}_L (cf. Corollary 1). This leads to a reduction of the worst-case complexity of the search space.

As an example, a contraction map which proves validity of (4.2) is shown in Table 1.⁶ One easily checks that occurrence vectors are respected, e.g. for $3 \in [n]$ we have $(0, 1, 1) \mapsto (0, 0, 1, 1)$, which matches (4.6). Iterating through every pair of rows, one can also check that the contraction property holds. Here the vectors defining the distance function are $\alpha = (1, 1, 1)$ and $\beta = (1, 1, 1, 1)$ for left and right, respectively. For instance, occurrence vectors 1 and 3 in the domain give $d_\alpha(x^{(1)}, x^{(3)}) = 1 + 0 + 1 = 2$, while their images $d_\beta(f(x^{(1)}), f(x^{(3)})) = 1 + 0 + 1 + 0 = 2 \leq d_\alpha(x^{(1)}, x^{(3)})$. Notice that the map f need not be injective nor surjective.

The proof of Theorem 4 is constructive and, as shown in [1], leads to an algorithm for finding a contraction map or showing none exists. The enumeration of all contraction maps is prohibitively expensive in all but very small cases. However, the authors developed a greedy technique for partial search which is successful in finding a map, when one exists. Indeed, we have found this method very powerful in proving new inequalities valid for H_6 . For proving an

⁶In fact, this contraction map which proves (4.2) is unique. This is generically not the case for larger- n facets, for which there usually exists many contraction maps compatible with the requirements of Theorem 4.

	S_{12}	S_{13}	S_{23}	S_1	S_2	S_3	S_{123}
0	0	0	0	0	0	0	0
	0	0	1	0	0	0	1
	0	1	0	0	0	0	1
3	0	1	1	0	0	1	1
	1	0	0	0	0	0	1
2	1	0	1	0	1	0	1
1	1	1	0	1	0	0	1
	1	1	1	0	0	0	1

Table 1: Representation of the contraction map which proves the MMI inequality (4.2). The left-most column labels the occurrence vectors shown in (4.6), including the one for $N \sim 0$. The top row labels bitstring entries, separating domain (left) from codomain (right). For the domain, S_{I_l} labels entries x_l , $l \in [L]$ for $x \in Q_L$ and, for the codomain, S_{J_r} labels entries y_r , $r \in [R]$ for $y \in Q_R$. Every row represents one entry of the map $f : x \mapsto y$ by listing all entries as $\{x, y\}$.

inequality is invalid, the previously-mentioned ILP approach, which will be presented in Section 5, is also very effective.

Theorem 4 provides a robust sufficient condition for an inequality to be valid, but it is not a necessary one. For example, even after exhausting all of the possibilities given by the theorem, it was not able to prove the validity of this inequality over H_5 :

$$\begin{aligned}
& 3S_{123} + 3S_{124} + S_{125} + S_{134} + 3S_{135} + S_{145} + S_{234} + S_{235} + S_{245} + S_{345} \geq \\
& 2S_{12} + 2S_{13} + S_{14} + S_{15} + S_{23} + 2S_{24} + 2S_{35} + S_{45} + 2S_{1234} + 2S_{1235} + S_{1245} + S_{1345}.
\end{aligned} \tag{4.19}$$

However, this inequality can be proved valid by expanding the codomain of f by replacing coefficients greater than one on the right-hand side by a sum of terms with unit coefficients. For instance, a term like $2S_I$ gets replaced by $S_I + S_I$, with the obvious generalization applied to larger coefficients. Theorem 4 still applies and this time the desired contraction map does exist, thereby proving validity of (4.19). By expanding the right-hand side there are more possible images for the contraction map, while the number of contraction conditions remains fixed. This may explain why this approach worked well here and in other cases we have tried for larger n .

This mild generalization of the proof technique of Theorem 4 has been remarkably successful in proving inequalities for $n = 6$, which motivates the following problem:

Problem 3. In (4.1), if we replace terms $\beta_r S_{J_r}$ with $\beta_r \geq 2$ by $\sum_{i=1}^{\beta_r} S_{J_r}$ and accordingly adjust R to $\sum_{r=1}^R \beta_r$, does Theorem 4 provide a necessary condition for validity over H_n ?

4.2 Zero-lifting of valid inequalities and facets

Given an inequality $qS \geq 0$ over H_n , let $K \subseteq [n]$ be the subset of terminals appearing in it. Then consider a family of disjoint, non-empty subsets $\{I_i \subseteq [n+1]\}_{i \in K}$ (not necessarily spanning). The *zero-lifting* of the inequality given by this family is obtained by replacing each singleton $i \in I$ in every S_I in $qS \geq 0$ by its corresponding I_i . For example, the zero-lifting of $S_1 + S_2 \geq S_{12}$ from H_3 to H_4 corresponding to $I_1 = \{2, 3\}$ and $I_2 = \{1, 4\}$ yields $S_{23} + S_{14} \geq S_{1234}$. The zero-lift where $I_i = \{i\}$ for every $i \in K$ is called the *trivial zero-lift*.

Proposition 6. *If an inequality $qS \geq 0$ is valid for H_n , then any zero-lift $q'S' \geq 0$ is valid for H_{n+1} .*

Proof. Assume $qS \geq 0$ is valid for H_n . Proceed by contradiction by supposing q has a zero-lift $q'S'$ such that $q'S' < 0$ for some $S' \in H_{n+1}$. Such S' must be realized by some weight map w

applied to K_N for some N . In this K_N , contract each terminal set I_i to the vertex in I_i with the minimum label, combining parallel edges and summing their weights into a single edge, and deleting any loops. Let S be the realized S -vector in the new graph. We have $q'S' = qS \geq 0$, the desired contradiction. \square

Before discussing lifting facets we need to recall some terminology from Proposition 1, in particular the weighted star graphs and the construction of matrix A^{n+1} in (2.6). We will make frequent use of the square matrix D^n of size $2^n - 1$, defined by

$$D_{I,J}^n = |I \cap J|, \quad \emptyset \neq I \subseteq [n], \quad \emptyset \neq J \subseteq [n+1], \quad n+1 \in J, \quad (4.20)$$

and use the notation D_J^n to refer to row J of D^n . An inequality $qS \geq 0$ in $\mathbb{R}^{2^n - 1}$ is called *balanced* if $D_{\{j\}}^n q = 0$ for all $j \in [n]$. By definition, balance is invariant under any permutation of terminals $[n]$, but need not be so under permutations of the extended terminals $[n; N]$. For instance, $S_1 + S_2 \geq S_{12}$ is balanced but $S_1 + S_{12} \geq S_2$ is not. Balance is equivalent to a seemingly stronger condition:

Lemma 3. *An inequality $qS \geq 0$ in $\mathbb{R}^{2^n - 1}$ is balanced if and only if $D^n q = 0$.*

Proof. Obviously, $D^n q = 0$ implies balance. For the converse, writing out row J of $D^n q$,

$$D_J^n q = \sum_{\emptyset \neq I \subseteq [n]} q_I |I \cap J| = \sum_{j=1}^n \delta_J^j \sum_{\emptyset \neq I \subseteq [n]} q_I \delta_I^j = \sum_{j=1}^n \delta_J^j D_{\{j\}}^n q, \quad (4.21)$$

where $\delta_I^i = \delta(i \in I)$ (cf. (4.5)) and we used $|I \cap J| = \sum_{k=1}^n \delta_I^k \delta_J^k$. So $D^n q = 0$ by balance. \square

What follows is a new result which relates the trivial zero-lifting of facets to the notion of balance:

Proposition 7. *If $qS \geq 0$ is a balanced facet of H_n , then its trivial zero-lift $q'S' \geq 0$ is a balanced facet of H_{n+1} .*

Proof. Suppose $qS \geq 0$ is a balanced facet of H_n . Then it is a valid inequality of H_{n+1} by Proposition 6. We adopt the notation of Proposition 1 and build a matrix A^{n+1} with the structure in (2.7), except it will now have only $2^{n+1} - 2$ rows. Let B^n consist of $2^n - 2$ linearly independent roots of $qS \geq 0$ as rows, so that the first $2^n - 2$ rows of A^{n+1} become precisely their zero-lifts. The trivial zero-lift has $q'_I = 0$ for every $I \ni n+1$, so these are all roots of $q'S' \geq 0$ as well. Since $qS \geq 0$ is balanced we have $D^n q = 0$ by Lemma 3. So the corresponding rows of A^{n+1} are roots of $q'S' \geq 0$ too. The final row is also and so A^{n+1} contains $2^{n+1} - 2$ roots of $q'S' \geq 0$. Performing the same column operations as in Proposition 1, the resulting block matrix (cf. \tilde{A}^{n+1}) shows that A^{n+1} has maximal rank $2^{n+1} - 2$. Since $D_{\{j\}}^{n+1} q' = D_{\{j\}}^n q = 0$, the lifted facet is also balanced. \square

The following proposition clarifies the situation for subadditive inequalities, which include the non-balanced Araki-Lieb inequalities in their orbits:

Proposition 8. *For all $n \geq 2$, a zero-lift of a subadditive inequality (2.15) gives a facet if and only if, using the symmetry $S_{[n;N] \setminus I} = S_I$, it can be put in the singleton SA form*

$$S_i + S_j \geq S_{ij}, \quad i \neq j \in [n; N]. \quad (4.22)$$

Proof. Since singleton SA is a balanced facet of H_2 , so is $S_i + S_j \geq S_{ij}$ for H_n by Proposition 7, as it can be obtained by iterating trivial zero-lifts and making a Sym_n permutation at the end.

For the converse, if a subadditive inequality is not in the form (4.22), we may write it as $S_I + S_{JK} \geq S_{IJK}$, for non-empty subsets I, J and K . This inequality is the sum of three valid inequalities for H_n : the general SA inequality (2.15), the general MMI inequality (4.3) and $S_I + S_K \geq S_{IK}$. Therefore, it is not a facet of H_n . \square

Apart from nonnegativity and the Araki-Lieb inequality associated to (4.22), all known facets of H_n are balanced. While balance is sufficient for trivial zero-lifts to preserve facets, a stronger condition is needed for general zero-lifts. A balanced inequality $qS \geq 0$ is *superbalanced* if every inequality in its symmetry orbit under Sym_{n+1} permutations of $[n; N]$ is balanced [13, 18]. Since balance is invariant under permutations of $[n]$, it is in fact only necessary to check if exchanges of every $i \in [n]$ with N yield balanced inequalities. Orbits of superbalanced inequalities are referred to as superbalanced. For example, SA in (2.15) for $I, J \subseteq [n]$ is balanced but not superbalanced and MMI in (4.2) is superbalanced. According to results stated in [13], besides the singleton SA orbit, every orbit of facets of H_n for $n \geq 2$ is superbalanced.

We can now generalize Proposition 7 to arbitrary zero-lifts. For an inequality $qS \geq 0$ in \mathbb{R}^{2^n-1} , let

$$\tilde{q}_I = \sum_{I \subseteq J \subseteq [n]} q_J. \quad (4.23)$$

Lemma 4. *An inequality $qS \geq 0$ in \mathbb{R}^{2^n-1} is superbalanced if and only if $\tilde{q}_I = 0$ for every $I \subseteq [n]$ with $|I| \leq 2$.*

Proof. That $\tilde{q}_{\{i\}} = 0$ for all $i \in [n]$ is just the definition of balance, which is an invariant property under permutations of $[n]$. Permutations of $[n; N]$ also allow for reflections $j \leftrightarrow N$ for each $j \in [n]$. Using $S_{[n; N] \setminus K} = S_K$, the S -vector entries S'_I after reflection are related to the S_I before reflection by $S'_J = S_J$ and $S'_{J \cup \{j\}} = S_{[n] \setminus J}$ for $J \not\ni j$. For example, $1 \leftrightarrow N$ for $n = 3$ gives $S' = (S_{123}, S_2, S_3, S_{13}, S_{12}, S_{23}, S_1)$. The coefficients q_I in $qS \geq 0$ behave accordingly. Under a $j \leftrightarrow N$ reflection, (4.23) gives $\tilde{q}'_{\{j\}} = \tilde{q}_{\{j\}}$, while for $i \neq j$ one gets

$$\tilde{q}'_{\{i\}} = \sum_{i \in J \subseteq [n] \setminus \{j\}} (q'_{J \cup \{j\}} + q'_J) = \sum_{i \in J \subseteq [n] \setminus \{j\}} (q_{[n] \setminus J} + q_J) = \sum_{j \in J \subseteq [n] \setminus \{i\}} q_J + \sum_{i \in J \subseteq [n] \setminus \{j\}} q_J. \quad (4.24)$$

The first sum is over all q_J such that $J \ni j$ but $J \not\ni i$, so it differs from \tilde{q}_j precisely by $\tilde{q}_{\{i, j\}}$. Similarly for the second sum exchanging $i \leftrightarrow j$, so

$$\tilde{q}'_{\{i\}} = \tilde{q}_{\{i\}} + \tilde{q}_{\{j\}} - 2\tilde{q}_{\{i, j\}}. \quad (4.25)$$

After the exchange $j \leftrightarrow N$, $q'S \geq 0$ is balanced if and only if $\tilde{q}'_{\{i\}} = 0$ for all $i \in [n]$. Therefore $qS \geq 0$ is superbalanced if and only if $\tilde{q}_{\{i\}} = \tilde{q}'_{\{i\}} = 0$ for all $i \in [n]$. Applied to (4.25), this means $qS \geq 0$ is superbalanced if and only if $\tilde{q}_{\{i\}} = \tilde{q}_{\{i, j\}} = 0$ for all $i, j \in [n]$. \square

We now show that any zero-lift of a superbalanced facet can actually be built solely out of trivial zero-lifts combined with permutations of the extended terminals, both of which preserve facets. Superbalance is needed for such permutations to preserve balance and thus keep Proposition 7 applicable. It is also important in what follows that, as is clear from Lemma 4 and the form of (4.23), balance and superbalance are properties which are shared by inequalities related by trivial zero-lifts. We first observe that the trivial zero-lift from H_n to H_{n+1} can be thought of as treating the new terminal $n + 1$ as a duplication of the sink (since the sink does not appear anywhere in $qS \geq 0$, neither does $n + 1$ in $q'S' \geq 0$). But by the symmetry of H_n

under Sym_{n+1} permutations of $[n; N]$, we could analogously consider letting $n+1$ duplicate any other terminal. Let us call such a generalization of a trivial zero-lift where any one extended terminal becomes a doubleton and the rest remain singletons a *simple zero-lift*. We obtain the following novel result:

Theorem 5. *If $qS \geq 0$ is a superbalanced facet of H_n , then any zero-lift $q'S' \geq 0$ is a superbalanced facet of H_{n+1} .*

Proof. If $qS \geq 0$ is a facet inequality over H_n involving a subset of terminals K with $|K| < n$, then put it in canonical form as an inequality over $H_{|K|}$. Iterating Proposition 5, note that $H_{|K|}$ is a projection of H_n . Since q is in canonical form, its coefficients are not changed in projecting it to $H_{|K|}$. A standard result of polyhedral theory is that facets project to facets, so $qS \geq 0$ is a superbalanced facet of $H_{|K|}$.

Starting from $qS \geq 0$, one can get to $q'S' \geq 0$ as follows. If the original zero-lift had $\{i\} \mapsto I_i$, perform $|I_i| - 1$ simple zero-lifts appending terminals to i , and repeat for every $i \in [n]$. If less than $n + 1 - |J|$ steps were required, reach all the way to H_{n+1} via trivial zero-lifts. At that point, a suitable permutation of $[n + 1]$ yields $q'S' \geq 0$.

We now show that every simple zero-lift used above can in fact be built solely out of permutations and trivial zero-lifts. In particular, the simple zero-lift involving $I_i = \{i, j\}$ is equivalently accomplished by exchanging $i \leftrightarrow N$, performing a trivial zero-lift, and then exchanging the new sink back with i . If the original inequality is superbalanced, the trivial zero-lift in this process is applied to a balanced inequality. Using Proposition 7, one ends up with a facet if one started with a facet. Furthermore, the latter is superbalanced if the former is. Hence one can go from $qS \geq 0$ to $q'S' \geq 0$ via superbalance- and facet-preserving steps. \square

5 Integer programs for testing realizability and validity

This section describes novel methods for checking if an S -vector is realizable (and if so finding a graph realization), and for checking if a given inequality is valid. A direct test of the realizability of an S -vector in K_N can be performed by a feasibility test of a mixed integer linear program (ILP). Similarly, an inequality $qS \geq 0$ can be tested to see if it is valid for all S -vectors that can be realized in K_N . As noted earlier, the polyhedral approach described so far does not force the minimum in (2.2) to be realized by one of the inequalities (3.1a). However, using binary variables this can be achieved and the feasibility of the resulting system tested using ILP solvers such as CPLEX, glpsol or Gurobi.

For any $N > n \geq 3$, we build a set of constraints, $ILP_{N,n}$, whose feasible solution is the set of all suitably-normalized, valid (S, w) pairs on n terminals realizable in K_N . Firstly, note that for each $\emptyset \neq I \subseteq [n]$, the number of cuts W in K_N that contain I is $2^{N-|I|-1}$. For each such W and I , we introduce a binary variable $y_{W,I}$. Specifically, we consider the following system:

ILP_{N,n}

For all $\emptyset \neq I \subseteq [n]$ and cuts $W \subseteq [N - 1]$ in K_N such that $I = W \cap [n]$,

$$S_I \leq \|C(W)\|, \tag{5.1}$$

$$\|C(W)\| \leq S_I + |W| (N - |W|) y_{W,I}, \tag{5.2}$$

$$\sum_{W \cap [n] = I} y_{W,I} = 2^{N-|I|-1} - 1, \tag{5.3}$$

$$y_{W,I} \in \{0, 1\}, \tag{5.4}$$

$$0 \leq w(e) \leq 1, \quad \forall e \in E_N. \tag{5.5}$$

Proposition 9. *A pair (S, w) is valid in K_N with all edge weights at most one if and only if there exists assignments to variables y so that $\{S, w, y\}$ is a feasible solution to $\text{ILP}_{N,n}$.*

Proof. Suppose that (S, w) is a valid pair in K_N with all edge weights at most one. We will show that y variables can be chosen so that $\{S, w, y\}$ constitutes a feasible solution to $\text{ILP}_{N,n}$. Firstly, by assumption w satisfies (5.5). Next, since (S, w) is a realization in K_N , the upper bounds in (5.1) are valid. For each $\emptyset \neq I \subseteq [n]$, choose one $W_I \subseteq [N-1]$ so that W_I realizes a minimum in (2.2), and set $y_{W_I, I} = 0$. All other y variables for this I are set to 1, thus satisfying (5.3) and (5.4). Since $y_{W_I, I} = 0$, the corresponding equation (5.2) gets zero as the second term in its right-hand side, and thus combines with (5.1) into the required equation. The remaining inequalities to verify are those in (5.2) when $y_{W, I} = 1$. Their validity follows from the fact that the cut W in K_N contains $|W|(N - |W|)$ edges, each of weight at most one.

Conversely, let $\{S, w, y\}$ be a feasible solution of $\text{ILP}_{N,n}$. For each $\emptyset \neq I \subseteq [n]$, (5.3) implies that there is a single variable, which we label $y_{W_I, I}$, having value zero. The other y values for this I are one. Together with (5.1), this implies that $S_I = \|C(W_I)\|$ and that S_I satisfies (2.2). So (S, w) is a valid pair realized in K_N with all edge weights at most one. \square

We make use of this ILP formulation in two ways. Firstly, it can be used to test whether or not an S -vector is realizable in K_N for a given N . To do this, we pre-assign the values from the given S -vector to the corresponding S variables in $\text{ILP}_{N,n}$, rescaled to values smaller than 1. We may then run an ILP solver to test whether there is a feasible solution. If so, the values or the variables w will give a realization in K_N . Otherwise, one concludes that the given S -vector cannot be represented in any $K_{N'}$ with $N' \leq N$. Secondly, we may use the ILP to test whether an inequality $qS \geq 0$ is invalid for some S -vector realized in K_N for a given N . This can be done by minimizing $z = qS$ over $\text{ILP}_{N,n}$ and seeing if the optimum solution is negative. The computation can be terminated when the first feasible solution with $z < 0$ is found, at which point $qS \geq 0$ is proven invalid. We could prove that an inequality $qS \geq 0$ is valid over H_n by testing it with $\text{ILP}_{m(n),n}$, but this ILP would be very large with current bounds on $m(n)$.

In its first formulation, the ILP allows one to find the minimum value N_{min} of N for which an S -vector is realizable in K_N . Given an S -vector, we call any such $K_{N_{min}}$ a *minimum realization*. At fixed n , we define $m_{ext}(n)$ as the smallest integer such that all extreme rays of H_n , and hence of $H_{m_{ext}(n),n}$, are realizable in $K_{m_{ext}(n)}$ (cf. the definition of $m(n)$). For $1 \leq n \leq 5$, the ILP shows that $m_{ext}(n)$ is

$$2, 3, 5, 6, 11. \tag{5.6}$$

Combining all extreme-ray graphs into a larger one by identifying them all at $[n; N]$ (cf. conically combining S -vectors), one can also see that for $1 \leq n \leq 3$, $m(n)$ takes values 2, 3 and 5. Namely, no bulk vertices are needed for $n = 1, 2$, and just a single one comes into play for $n = 3$.

The case $n = 4$ is less trivial. There are two star-graph orbits of 5 extreme rays each, see Figure 1 in Appendix B.2. These are 10 extreme rays realizable in K_6 , which contains a single bulk vertex. The other extreme rays of H_4 involve no bulk vertices. Hence, a convex combination of 15 extreme rays may require a total of 10 bulk vertices at most, which with the terminals and sink gives $m(4) \leq 15$. This can be further improved as follows. The Bell-pair extreme rays span a subspace of dimension 10, and the star-graph extreme rays are confined to its 5-dimensional orthogonal complement. Thus at most 5 star-graph extreme rays are needed to conically span any interior ray of H_4 , improving the bound down to $m(4) \leq 10$. It turns out that the simplicity of the specific extreme-ray graphs for $n = 4$ in fact allows us to obtain the definite value $m(4) = 6$. The reason for this is that the S -vector of any conical combination of these particular extreme-ray star graphs of H_4 can itself also be realized on a star graph. This follows from the observation that all $n = 4$ extreme-ray star graphs have identical minimal

min-cuts: for every $\emptyset \neq I \subseteq [n]$, they all have $W_I = I$ for $|I| = 1, 2$ and $W_I = I \cup \{n\}$ for $|I| = 3, 4$. Pictorially, this allows one to stack them all on top of each other, adding up their edge weights, so as to realize any combination of these star graphs by a star graph.

This discussion illustrates some strategies for obtaining tighter upper bounds on $m(n)$ based on knowledge of extreme rays or the value of $m_{ext}(n)$. Recall that the number of bulk vertices in K_N is $N - n - 1$. Regardless of how many extreme rays H_n has, any interior ray may be a conical combination of at most $2^n - 1$ of them. Since we can realize all extreme rays in $K_{m_{ext}(n)}$, we have

$$m(n) \leq (m_{ext}(n) - n - 1) \times (2^n - 1) + n + 1. \quad (5.7)$$

For instance, since we know $m_{ext}(5) = 11$, this gives $m(5) \leq 161$, which is considerably better than the bound $m(5) < M(5) = 2546$ given earlier.

We can do even better for $n = 5$ by using explicit results about the dimensionality of the span of specific extreme-ray orbits. The Bell pairs take care of 15 dimensions which are not reached by any other extreme ray without introducing any bulk vertices. There is a single orbit that requires $N = 11$, and it consists of 75 extreme rays spanning a subspace of dimension 10 of the remaining 16 of $H_5 \subset \mathbb{R}^{31}$. The largest- N orbit spanning the other 6 dimensions has $N = 8$ and 360 extreme rays. Hence the worst-case scenario would require 10 graphs with $N = 11$ and other 6 with $N = 8$. The total number of vertices carried by a combination of such graphs thus gives the bound $m(5) \leq 74$. This is better than the more general one attained by (5.7), but requires complete knowledge of all extreme-ray graphs, not just of the number $m_{ext}(n)$.

Problem 4. Find tighter bounds on $m_{ext}(n)$. In particular, does $\log_2 m_{ext}(n)$ admit an upper bound that is polynomial in n ?

6 Computing H - and V -representations of H_n

To date, there existed no direct or algorithmic procedures for constructing H_n , and all results obtained for up to $n = 5$ relied on random/heuristic searches. This section provides two novel systematic methods for computing complete descriptions of H_n . We illustrate them for $n = 5$ and describe H_5 in detail in Appendix B.⁷ We also show how partial results for $n = 6$ can be obtained by our methods. However, a complete description of H_6 appears to be beyond current computational capabilities. Further upgrading our methods to obtain H_6 is the subject of work in progress with Bogdan Stoica, to be reported elsewhere. The first method is a general formalization of the strategy used earlier for $n = 3, 4$, whereas the second one constructs H_n starting from knowledge of H_{n-1} .

6.1 Method 1

To initialize this method we first set $k = 2$.

Method 1

-
- (a) Generate the H -representation $P\{\mathbf{n+k}\}\text{-n.in}$ of $P_{n+k,n}$ using (3.1). Convert this to a V -representation $P\{\mathbf{n+k}\}\text{-n.ext}$.
 - (b) Delete the $2^n - 1$ trivial extreme rays (see Theorem 2) and extract the $2^n - 1$ coordinates corresponding to the variables of the S -vectors. Remove redundant

⁷A partial description of H_5 was first obtained by [1] and only four years later completed by [14]; the approaches proposed here only take a few hours and additionally obtain provably minimum graph realizations of all extreme rays unknown to date.

rays to obtain the V -representation $H\{n+k\}-n.\text{ext}$ of $H_{n+k,n}$. This is an inner approximation of H_n .

- (c) Compute the H -representation $H\{n+k\}-n.\text{ine}$ of $H_{n+k,n}$ from $H\{n+k\}-n.\text{ext}$. Using the ILP method with of Section 5 with $N \geq n + 1$, reject facet orbits that are invalid for K_N , continuing until either a facet is rejected or N is too large for the ILP to solve.
- (d) Test any remaining facet orbits for which the validity is unknown using the proof-by-contraction method of Section 4.1. Generate the full orbits of the facets proved valid, getting a cone $HV\{n+k\}-n.\text{ine}$ which is an outer approximation of H_n .
- (e) Compute the extreme rays $HV\{n+k\}-n.\text{ext}$ of $HV\{n+k\}-n.\text{ine}$. The orbits of S -vectors that appeared in $P\{n+k\}-n.\text{ext}$ give extreme rays of H_n by Theorem 2(b). The remaining orbits can be checked by the ILP method of Section 5 with $N \geq n + 1$ until finding a realization or N being too large for the ILP to solve. If all extreme-ray orbits can be realized, then $HV\{n+k\}-n.\text{ine}$ is an H -representation of H_n and $HV\{n+k\}-n.\text{ext}$ is its V -representation by Proposition 2(c). Otherwise, increment k and return to step (a).

Applying Method 1 with $n = 5$, one finds that $P_{7,5}$ has 83 facets and 194 extreme rays in 52 dimensions. The resulting $H_{7,5}$ has 142 extreme rays in 31 dimensions, and its H -representation consists of 8952 facets in 30 orbits. All but 8 of them are easily eliminated in step (c) and then proved valid in step (d). These orbits give 372 facets which define $HV7-5.\text{ine}$. Correspondingly, $HV7-5.\text{ext}$ has 2267 extreme rays falling into 19 orbits. All of the extreme rays are realizable for $N \leq 11$, so the procedure terminates after a single iteration. Note that we obtain a minimum realization of each extreme ray either in step (a) or (e), wherever it appears first.

The vertex/facet enumeration problems in steps (a), (c) and (e) utilized the code `Normaliz`⁸ *v.3.4.1* on `mai20`⁹. Steps (a) and (c) took only a few seconds, and step (e) took 23 minutes. Step (d) was run on a laptop¹⁰ using a `Mathematica v.12.1` implementation¹¹ of the proof-by-contraction method. Most runs were very fast, taking less than 4 seconds, and all finished in no more than 16 minutes. The ILP runs in step (e) were performed with `CPLEX`¹² *v.12.6.3*, also on `mai20`, and normally completed in under 1 minute, the longest run taking 18 minutes. The filtration by symmetry generally takes just a few seconds.

Applying Method 1 with $n = 6$ we run into computational issues as the vertex/facet enumeration problems quickly become too big to solve with current software and hardware. Nevertheless, we are still able to get useful results using only partial computations. Starting with $k = 2$, $P_{8,6}$ has 154 facets and 194 extreme rays in 91 dimensions. The resulting V -representation of $H_{8,6}$ has 4361 extreme rays in 63 dimensions falling into 21 orbits. All 21 orbits can be shown to define orbits of extreme rays of H_6 by testing their rank against lifts of $n = 5$ inequalities to $n = 6$. Obtaining the H -representation of $H_{8,6}$ is computationally intractable with presently available algorithms and hardware. To get more extreme ray orbits we set $k = 3$ and constructed the H -representation of $P_{9,6}$, which has 288 facets in 99 dimensions. It was not possible to do a complete computation of it V -representation. The code `Normaliz` ran out of memory after about a day of computation, as did other double-description based methods. However we were able

⁸<https://www.normaliz.uni-osnabrueck.de>

⁹`mai20`: 2× Xeon E5-2690 (10-core 3.0GHz), 20 cores, 128GB memory.

¹⁰Dell XPS 15 7590, i7-9750H CPU @ 2.60GHz, 6 cores, 12 threads, 32GB memory.

¹¹Available upon request.

¹²<https://www.ibm.com/analytics/cplex-optimizer>

to get partial results using the parallel reverse search based method `mplrs` contained in `lrslib`¹³ *v.7.2* which gives output in a stream. After about 6 months of computation with `mplrs` using between 100 and 200 processors we obtained 213,225 extreme rays which fall into 1066 orbits. By construction, all of these extreme rays are realizable in K_9 . Together, these orbits generate about 3 million extreme rays, however 460 orbits become redundant when the full orbits are considered. The 606 non-redundant orbits generate about 1.5 million extreme rays and 402 of the orbits are provably orbits of extreme rays of H_6 using lifted inequalities from $n = 5$. Unfortunately it is not possible to compute the facets of such a large cone with current methods. It is important to note that `mplrs` supports checkpoint/restart and continuing the computation will continue the output stream until a complete V -representation is obtained. Being based on reverse search, computer memory is not a constraining factor.

6.2 Method 2

The second method is more sophisticated and involves working with both outer and inner approximations of H_n , refining them until they are equal. The outer approximation is initialized by choosing any set of valid inequalities for H_n , not necessarily facets, whose intersection is full dimensional. The inner approximation is initialized by choosing any feasible set of rays, not necessarily extreme, whose convex hull is also full dimensional. A strong way to initialize the outer approximation is to zero-lift the superbanded facets of H_{n-1} in all possible ways, add to them singleton SA, and generate their full orbits under Sym_{n+1} . By Theorem 5 and Proposition 8, these are all facets of H_n and define a cone `OH1-n.ine`. For a strong inner approximation, we zero-lift the extreme rays of H_{n-1} and generate their full orbits under Sym_{n+1} , which are all extremal in H_n by Proposition 5. Since this is not always full-dimensional, we add the full orbits of the S -vectors from Proposition 1 not already included, and remove redundancies. In general, this may only add the single orbit of size $n + 1$ generated by $S^{[n]}$. The resulting cone `IH1-n.ext` is an inner approximation of H_n . Set the iteration counter $k = 1$.

Method 2

Outer	Inner
Compute the V -representation <code>OHk-n.ext</code> of <code>OHk-n.ine</code> . Check one extreme ray from each orbit to see if it is realizable by the ILP method of Section 5. If all rays are realizable, then exit . The full orbits of the realizable extreme rays define <code>OHVk-n.ext</code> .	Compute the H -representation <code>IHk-n.ine</code> of <code>IHk-n.ext</code> . Apply to it steps (c) and (d) of Method 1, retaining inequalities proved by the contraction method of Section 4.1. If all inequalities are valid, then exit . The full orbits of the valid facets define <code>IHVk-n.ine</code> .
↓	↓
Merge <code>IHVk-n.ine</code> (and any other known valid inequalities) with <code>OHk-n.ine</code> and remove redundancies to get <code>OH{k+1}-n.ine</code> .	Merge <code>OHVk-n.ext</code> (and any other known realizable rays) with <code>IHk-n.ext</code> and remove redundancies to get <code>IH{k+1}-n.ext</code> .
↓	↓
Increment k and return to the first step of each respective subroutine.	

Note that the inner and outer procedures can be run in parallel. After they both finish

¹³<http://cgm.cs.mcgill.ca/~avis/C/lrs.html>

the first step, the newly computed data are exchanged, improving both the outer and inner approximations. If `exit` occurs, the corresponding `ine` and `ext` descriptions give H - and V -representations of H_n , respectively. In each subroutine, the second step allows for the incorporation of valid inequalities and/or rays obtained by other means, such as Method 1.

Applying Method 2 with $n = 5$, the starting cones `OH1-5.ine` and `IH1-5.ext` respectively consist of 80 facets in 3 orbits (that of singleton SA and 2 of MMI, cf. Appendix B.1), and 66 extreme rays in 4 orbits (cf. Figure 1 in Appendix B.2, and the $J = [n]$ star orbit).

We start with $k = 1$ and describe steps in parallel. In the outer run, `OH1-5.ext` has 3205 extreme rays in 29 orbits, out of which 16 can be shown to be realizable with $N \leq 11$. Their orbits yield 1457 feasible rays defining `OHV1-5.ext`. In the inner run, `IH1-5.ine` has 157153 facets in 346 orbits, out of which one can show 8 are valid and easily reject the rest. Their orbits yield 372 valid inequalities defining `IHV1-5.ine`. In the second step it turns out that the outputs of the first step dominate in both cases. So after the merges, `OH2-5.ine` equals `IHV1-5.ine` and `IH2-5.ext` equals `OHV1-5.ext`.

Setting $k = 2$, in the outer run `OH2-5.ext` has 2267 extreme rays in 19 orbits, all of which are realizable with $N \leq 11$. Hence `exit` is triggered, and the algorithm terminates returning `OH2-5` as the result for H_5 . If we continue the inner run we find that `IH2-5.ine` has 1182 facets in 11 orbits, out of which one can show 8 are valid and easily reject the rest. These are the same 8 orbits as before and so the algorithm exits in the first outer step with $k = 3$.

Conversions between cone representations again require vertex/facet enumeration. Those in the first iteration are immediate. Using `Normaliz` on `mai20`, the computations of `IH2-5.ine` and `OH3-5.ext` took about 75 seconds and 25 minutes, respectively. The cost of other computations was similar to that of their counterparts in Method 1.

Applying Method 2 with $n = 6$, the starting cones `OH1-6.ine` and `IH1-6.ext` are in 63 dimensions and respectively consist of 6503 facets in 11 orbits and 15617 extreme rays in 20 orbits. We start with $k = 1$. Again we have to be satisfied with partial computation using `mplrs` as the problem is too large for current computational methods to terminate in reasonable time. In the outer run after about 10 days of computation we obtained 3445 extreme rays from `OH1-6.ext` belonging to 3288 distinct orbits. None of these 3288 orbits can be ruled out using lifted inequalities (by construction, because they come from `OH1-6.ine`), which means a priori we have literally 3288 candidates. Using a set of heuristically generated inequalities that we were able to prove valid via the contraction method, we reduce this list down to 55 candidates. Of these, 5 orbits are easily seen to correspond to lifts of $n = 5$ extreme rays. Using `CPLEX` and the ILP method we found minimum realizations of all 55 orbits: 1 in K_7 (lift of a Bell pair), 6 in K_8 (4 are lifts of star graphs), 10 in K_9 , 13 in K_{10} , 16 in K_{11} and 9 in K_{12} . All of these extreme rays are thus extreme rays of H_6 by construction. Note that only those realizable in K_n for $n \leq 9$ could have appeared in the Method 1 run described. As noted for Method 1, the computation of `OH1-6.ext` can be continued with additional new orbits being produced as a stream until the computation is completed. In the inner run, the computation of the H -representation of `IH1-6.ext` was too big to produce any useful output in two weeks of computation with `mplrs` using 160 processors.

6.3 Comparison of Method 1 and Method 2

Although the inner steps of Method 2 may appear similar to Method 1, they are in fact quite distinct. In the latter, the starting cone `H{n+2}-n.ext` only contains S -vectors realizable in K_{n+2} . Many of these will be non-extremal in H_n and therefore absent from `IH1-n.ext`. Among those which are extremal, some may not be obtainable by zero-lift and thus not included in `IH1-n.ext` either. On the other hand, `IH1-n.ext` contains all extreme rays of H_n coming from

zero-lifts. These will generally include plenty which are not realizable in K_{n+2} and hence not be contained in $H\{n+2\}\text{-n.ext}$. For example, for $n = 6$, $IH1\text{-}6\text{-ext}$ includes zero-lifts of extreme rays in the 5 orbits of H_5 which are realizable in K_N with $N \geq 9$ (see Table 3 in Appendix B.2), none of which can possibly be in $H8\text{-}6\text{-ext}$.

Both methods may run into fundamental and/or practical issues. For $n = 5$, one is fortunate that the contraction method successfully proves valid the 8 facet orbits of H_5 . However, it remains a logical possibility that for larger n this proof method is not a necessary condition for validity of some facets of H_n (cf. Problem 3 at the end of Section 4.1). Specifically in Method 1, it so happens that all rays in $HV7\text{-}5\text{-ext}$ are realizable using the ILP of Section 5. For larger n , in practice it could be that even if all rays at step (e) were realizable, the value of N required could be too high for the ILP to be solved. Without good bounds on $m_{ext}(n)$, this possibility cannot be easily eliminated. Alternatively, it could be that some rays are indeed not realizable, meaning that the facet description in $HV\{n+k\}\text{-n.ine}$ is incomplete. This would require incrementing k and at least one further iteration. As for Method 2, we unfortunately have no proof of convergence using the strong starting inputs suggested without the option to generate and add additional valid inequalities and/or feasible rays in the second step. There are various heuristic methods available to generate such additional inputs. Another complication that affects these methods is the need to solve large convex hull/facet enumeration problems. All of these issues arise in one form or another in both methods already in the study of H_6 .

The successful termination of either method relies on the finding of an H/V -representation of an inner/outer approximation of H_n containing all of its facets/extreme rays. For instance, observe that in Method 1 all facets of H_5 were already discovered in step (a) and computed explicitly in step (c) (along with other non-valid inequalities) from $H_{N,5}$ for just $N = 7$. Similarly, Method 2 converged more easily through an inner approximation $IH1\text{-}5$ whose H -representation also contained all facets of H_5 . That H_n is easier to obtain from an H -representation of an inner approximation is no accident. This is because smaller N for K_N is needed to span all facets than to realize all extreme rays of H_n . This motivates the definition of $m_{ine}(n)$ as the smallest integer such that the H -representation of $H_{m_{ine}(n),n}$ contains all facets of H_n .

It is easily seen that $m_{ine}(n) = m_{ext}(n)$ for $1 \leq n \leq 4$ and that $m_{ine}(n) \leq m_{ext}(n)$ for larger n . For $n = 5$, the cone $H_{6,5}$ turns out to miss some facets of H_5 , but $H_{7,5}$ does contain them all as we have seen in Method 1. This shows that $m_{ine}(5) = 7$, contrasting with the extreme rays, which have $m_{ext}(5) = 11$. More generally, when Method 1 terminates, we have $m_{ine}(n) = n + k$ and a minimum realization of each extreme ray, from which one also obtains $m_{ext}(n)$. This makes the importance of $m_{ine}(n)$ manifest and motivates the following problem:

Problem 5. Find tighter bounds on $m_{ine}(n)$. In particular, does $\log_2 m_{ine}(n)$ admit an upper bound that is polynomial in n ?

7 Conclusion

Many of the important questions about the HEC remain open. As stated formally throughout the paper in Problems 1 through 5, these include obtaining an explicit description of either the H - or V -representation of H_n , and finding the complexity of testing feasibility of rays and validity of inequalities. The current bounds on the size of the complete graph that can realize all extreme rays of H_n seem far from being tight, at least according to the limited experimental results that we have. Similarly, our findings suggest that much smaller graphs may be sufficient to span all facets of H_n , which strongly motivates understanding better the relative complexity of the H - and V -representations of the HEC. Ultimately, one would hope to obtain a more fundamental understanding of the HEC, such as in the form of the structural conjectures put forward recently in [8–10, 16]. In this work, we have laid the foundations

for further exploration of these key questions and provided some useful tools for testing and proving such ideas. Additionally, we have provided sharp computational tools which allowed us to completely describe H_5 after just a few hours of computation and produce significant new results for H_6 .

Acknowledgments

We thank Patrick Hayden, Temple He, Veronika Hubeny, Max Rota, Bogdan Stoica and Michael Walter for useful discussions. We would also like to thank an anonymous referee for many comments and suggestions for improving the paper.

References

- [1] Bao N, Nezami S, Ooguri H, Stoica B, Sully J, Walter M (2015) The Holographic Entropy Cone. JHEP 09:130, doi:[10.1007/JHEP09\(2015\)130](https://doi.org/10.1007/JHEP09(2015)130), arXiv:[1505.07839](https://arxiv.org/abs/1505.07839)
- [2] Bao N, Cheng N, Hernández-Cuenca S, Su VP (2020) A Gap Between the Hypergraph and Stabilizer Entropy Cones. arXiv:[2006.16292](https://arxiv.org/abs/2006.16292)
- [3] Bao N, Cheng N, Hernández-Cuenca S, Su VP (2020) The Quantum Entropy Cone of Hypergraphs. SciPost Phys 9(5):067, doi:[10.21468/SciPostPhys.9.5.067](https://doi.org/10.21468/SciPostPhys.9.5.067), arXiv:[2002.05317](https://arxiv.org/abs/2002.05317)
- [4] Brouwer AE, Mills C, Mills W, Verbeek A (2013) Counting families of mutually intersecting sets. Electron J Comb 20(2), doi:[10.37236/2693](https://doi.org/10.37236/2693)
- [5] Chen B, Czech B, Wang Zz (2022) Quantum information in holographic duality. Rept Prog Phys 85(4):046001, doi:[10.1088/1361-6633/ac51b5](https://doi.org/10.1088/1361-6633/ac51b5), arXiv:[2108.09188](https://arxiv.org/abs/2108.09188)
- [6] Cunningham WH (1985) On submodular function minimization. Comb 5(3):185–192, doi:[10.1007/BF02579361](https://doi.org/10.1007/BF02579361)
- [7] Czech B, Dong X (2019) Holographic Entropy Cone with Time Dependence in Two Dimensions. JHEP 10:177, doi:[10.1007/JHEP10\(2019\)177](https://doi.org/10.1007/JHEP10(2019)177), arXiv:[1905.03787](https://arxiv.org/abs/1905.03787)
- [8] Czech B, Shuai S (2021) Holographic Cone of Average Entropies. arXiv:[2112.00763](https://arxiv.org/abs/2112.00763)
- [9] Czech B, Wang Y (2022) A holographic inequality for $N = 7$ regions. arXiv:[2209.10547](https://arxiv.org/abs/2209.10547)
- [10] Fadel M, Hernández-Cuenca S (2022) Symmetrized holographic entropy cone. Phys Rev D 105(8):086008, doi:[10.1103/PhysRevD.105.086008](https://doi.org/10.1103/PhysRevD.105.086008), arXiv:[2112.03862](https://arxiv.org/abs/2112.03862)
- [11] Fujishige S (2005) Submodular Functions and Optimization, Ann. Discrete Math., vol 58. Elsevier, doi:[10.1016/S0167-5060\(13\)71057-4](https://doi.org/10.1016/S0167-5060(13)71057-4)
- [12] Hayden P, Headrick M, Maloney A (2013) Holographic Mutual Information is Monogamous. Phys Rev D 87(4):046003, doi:[10.1103/PhysRevD.87.046003](https://doi.org/10.1103/PhysRevD.87.046003), arXiv:[1107.2940](https://arxiv.org/abs/1107.2940)
- [13] He T, Hubeny VE, Rangamani M (2020) Superbalance of Holographic Entropy Inequalities. JHEP 07:245, doi:[10.1007/JHEP07\(2020\)245](https://doi.org/10.1007/JHEP07(2020)245), arXiv:[2002.04558](https://arxiv.org/abs/2002.04558)
- [14] Hernández-Cuenca S (2019) Holographic entropy cone for five regions. Phys Rev D 100(2):026004, doi:[10.1103/PhysRevD.100.026004](https://doi.org/10.1103/PhysRevD.100.026004), arXiv:[1903.09148](https://arxiv.org/abs/1903.09148)
- [15] Hernández-Cuenca S, Hubeny VE, Rangamani M, Rota M (2019) The quantum marginal independence problem. arXiv:[1912.01041](https://arxiv.org/abs/1912.01041)
- [16] Hernández-Cuenca S, Hubeny VE, Rota M (2022) The holographic entropy cone from marginal independence. JHEP 09:190, doi:[10.1007/JHEP09\(2022\)190](https://doi.org/10.1007/JHEP09(2022)190), arXiv:[2204.00075](https://arxiv.org/abs/2204.00075)
- [17] Hubeny VE, Rangamani M, Rota M (2018) Holographic entropy relations. Fortsch Phys 66(11-12):1800067, doi:[10.1002/prop.201800067](https://doi.org/10.1002/prop.201800067), arXiv:[1808.07871](https://arxiv.org/abs/1808.07871)

- [18] Hubeny VE, Rangamani M, Rota M (2019) The holographic entropy arrangement. *Fortsch Phys* 67(4):1900011, doi:[10.1002/prop.201900011](https://doi.org/10.1002/prop.201900011), arXiv:[1812.08133](https://arxiv.org/abs/1812.08133)
- [19] Kleitman D, Markowsky G (1975) On Dedekind’s Problem: The Number of Isotone Boolean Functions. II. *Trans Am Math Soc* 213:373–390, doi:[10.2307/1998052](https://doi.org/10.2307/1998052)
- [20] Nezami S, Walter M (2020) Multipartite Entanglement in Stabilizer Tensor Networks. *Phys Rev Lett* 125:241602, doi:[10.1103/PhysRevLett.125.241602](https://doi.org/10.1103/PhysRevLett.125.241602), arXiv:[1608.02595](https://arxiv.org/abs/1608.02595)
- [21] Nielsen MA, Chuang IL (2010) *Quantum Computation and Quantum Information*. Cambridge University Press, doi:[10.1017/CBO9780511976667](https://doi.org/10.1017/CBO9780511976667)
- [22] Pippenger N (2003) The inequalities of quantum information theory. *IEEE Trans Inf Theory* 49(4):773–789, doi:[10.1109/TIT.2003.809569](https://doi.org/10.1109/TIT.2003.809569)
- [23] Rangamani M, Takayanagi T (2017) Holographic Entanglement Entropy, *Lect. Notes Phys.*, vol 931. Springer, doi:[10.1007/978-3-319-52573-0](https://doi.org/10.1007/978-3-319-52573-0), arXiv:[1609.01287](https://arxiv.org/abs/1609.01287)
- [24] Ryu S, Takayanagi T (2006) Holographic derivation of entanglement entropy from AdS/CFT. *Phys Rev Lett* 96:181602, doi:[10.1103/PhysRevLett.96.181602](https://doi.org/10.1103/PhysRevLett.96.181602), arXiv:[hep-th/0603001](https://arxiv.org/abs/hep-th/0603001)
- [25] Schrijver A (1999) *Theory of Linear and Integer Programming*. Wiley Series in Discrete Mathematics & Optimization, Wiley
- [26] Van Raamsdonk M (2010) Building up spacetime with quantum entanglement. *Gen Rel Grav* 42:2323–2329, doi:[10.1142/S0218271810018529](https://doi.org/10.1142/S0218271810018529), arXiv:[1005.3035](https://arxiv.org/abs/1005.3035)
- [27] Walter M, Witteveen F (2020) Hypergraph min-cuts from quantum entropies. arXiv:[2002.12397](https://arxiv.org/abs/2002.12397)

A Origins and importance of the HEC in physics

The tools of convex geometry have long been applied to systematically study entropy inequalities, from those obeyed by the Shannon entropy of random variables in classical probability distributions, to the ones that the von Neumann entropy of marginals of density matrices of quantum states satisfy [22]. As a measure of quantum entanglement, the study of the latter has proven to be of paramount importance to the development of the field of quantum information theory and, more generally, to the understanding of correlations in quantum physics [21].

Although the finding of universal inequalities obeyed by general quantum states has been elusive, significant progress has been made by the restriction of the domain of the entropy function to specific subclasses of quantum states of special relevance for which additional tools are at hand. In the context of quantum gravity and holography, one very important such class of quantum states are those which admit a semi-classical description in terms of a theory of gravity on a higher-dimensional spacetime. More specifically, in such cases, the Anti-de Sitter/Conformal Field Theory (AdS/CFT) correspondence asserts that a holographic state of the CFT, defined on a *boundary* spacetime M , has a gravitational *bulk* dual on a spacetime \mathcal{M} with M as its conformal boundary, $\partial\mathcal{M} = M$. In the bulk, quantum entanglement of the CFT state acquires a geometric character which has been understood to play a fundamental role in the very emergence of spacetime itself [26]. These findings rely on the much celebrated Ryu-Takayanagi (RT) prescription [23, 24], according to which the von Neumann entropy $S(R)$ of a spatial boundary region $R \subset M$ is given holographically by

$$S(R) = \min_{\mathcal{R} \subset \mathcal{M}} \frac{\text{area}(\mathcal{R})}{4G\hbar}, \quad (\text{A.1})$$

where G is Newton constant, \hbar is Planck constant, and the minimization is over bulk hypersurfaces \mathcal{R} in a time slice homologous to R relative to ∂R , i.e., subject to the condition $\partial\mathcal{R} = \partial R$. This geometric character that the von Neumann entropy acquires in the bulk turns out to place strong constraints on the allowed entanglement structures of holographic states. In a remarkable paper, Bao et al. [1] initiated a systematic exploration of these constraints with the objective of formalizing a set of conditions on quantum states to possess holographic duals. These were formulated as entropy inequalities satisfied by the RT formula, defining the facets of a polyhedral cone which was coined as the HEC.

More precisely, the HEC is a family of polyhedral cones H_n labelled by an integer $n \geq 1$, all related by projections from larger to smaller n . Their work laid the ground for the finding of new results about the HEC [7, 13, 14], and also lead to further generalizations and explorations of their methods [2, 3, 15, 17, 18, 27]. Most of these developments relied on two remarkable results of [1]: a proof of equivalence between holographic entropies obtained by the RT formula and minimum cuts on weighted graphs¹⁴, and the invention of a combinatorial method to prove the validity of holographic entropy inequalities that we will review in Section 4. Crucially, their graph models allow for a complete study of the HEC from a purely combinatorial viewpoint without reference to the geometric RT formula or quantum physics.

B Extremal structure of H_n for $1 \leq n \leq 5$

Here we summarize the extremal structure of H_n for all $1 \leq n \leq 5$ by showing representatives of every orbit of both facets and extreme rays. Representatives of each orbit are picked as their lexicographical minimum.¹⁵ For extreme rays, we also present their minimum realizations, exhibiting graphs where only edges of nonzero weight are shown. At every n , we only include elements which are genuinely new and not coming from zero-liftings. This is because these should always be included – by Proposition 5 the zero-lift of rays preserves all extreme rays, while by Theorem 5 the zero-lift of inequalities preserves all superbalanced facets. As for SA, Proposition 8 guarantees that precisely only instances involving just singletons in $[n; N]$ give rise to facets. It will thus be convenient to present results in increasing order of n .

B.1 Facets

At $n = 1$ one just has one single-element orbit of a nonnegativity facet,

$$S_1 \geq 0. \tag{B.1}$$

For $n = 2$, the cone is a simplex with 3 facets in a single orbit of SA,

$$S_1 + S_2 \geq S_{12}. \tag{B.2}$$

Lifting to $n = 3$, one gets 6 facets in the orbit of the trivial zero-lift of SA. The cone becomes again a simplex due to the appearance of the new, totally symmetric facet of MMI

$$S_{12} + S_{13} + S_{23} \geq S_1 + S_2 + S_3 + S_{123}. \tag{B.3}$$

There are no genuinely new inequalities for $n = 4$. The trivial zero-lift of the SA facet gives a length-10 orbit. Every zero-lift of (B.3) in fact lands on the same MMI orbit, which consists of another 10 facets. In total, H_4 thus has 20 facets and is not simplicial anymore.

¹⁴Intuitively, the graph provides a discrete tessellation of the manifold which encodes sufficient information about its metric in the form of edge weights, with minimal surfaces and their areas becoming minimum cuts and their weights, respectively – see [1].

¹⁵The only exception to this is inequality 1 in Table 2, which is chosen for symmetry reasons.

It is at $n = 5$ that H_n begins to exhibit a richer structure. The trivial zero-lift of SA now contributes an orbit of 15 facets. The trivial zero-lift of MMI gives an orbit with 20 facets. There is now another inequivalent zero-lift of MMI which gives an orbit of length 45. Besides these, there are 5 orbits of genuinely new facets, given in Table 2.

In order, these give rise to orbits of lengths 72, 90, 10, 60 and 60. Together with the 80 facets coming from SA and MMI, there are a total of 372 inequalities in the H -representation of H_5 . Other than inequality 1, usually referred to as *cyclic* due to its symmetry under $i \rightarrow i + 1 \pmod n$ which is manifest in the given representative, these inequalities are poorly understood.

<p>1. $S_{123} + S_{234} + S_{345} + S_{145} + S_{125} \geq S_{12} + S_{23} + S_{34} + S_{45} + S_{15} + S_{12345}$</p>	
<p>2. $S_{14} + S_{23} + S_{125} + S_{135} + S_{145} + S_{245} + S_{345} \geq S_1 + S_2 + S_3 + S_4 + S_{15} + S_{45} + S_{235} + S_{1245} + S_{1345}$</p>	<p>3. $S_{123} + S_{124} + S_{125} + S_{134} + S_{135} + S_{145} + S_{235} + S_{245} + S_{345} \geq S_{12} + S_{13} + S_{14} + S_{25} + S_{35} + S_{45} + S_{234} + S_{1235} + S_{1245} + S_{1345}$</p>
<p>4. $2S_{123} + S_{124} + S_{125} + S_{134} + S_{145} + S_{235} + S_{245} \geq S_{12} + S_{13} + S_{14} + S_{23} + S_{25} + S_{45} + S_{1234} + S_{1235} + S_{1245}$</p>	<p>5. $3S_{123} + 3S_{124} + S_{125} + S_{134} + 3S_{135} + S_{145} + S_{234} + S_{235} + S_{245} + S_{345} \geq 2S_{12} + 2S_{13} + S_{14} + S_{15} + S_{23} + 2S_{24} + 2S_{35} + S_{45} + 2S_{1234} + 2S_{1235} + S_{1245} + S_{1345}$</p>

Table 2: Representative inequalities in each of the 5 new orbits of facets of H_5 .

B.2 Extreme rays and minimum graph realizations

Extreme rays and their minimum realizations in $K_{N_{min}}$ will be provided. Extreme rays will be labelled by a tuple $(n, N_{min} - n, \sigma)$, where $\sigma \geq 1$ is just an integer counting orbits at fixed n and N_{min} by listing their representatives lexicographically. Notice that $N_{min} - n \geq 1$ counts the number of bulk vertices needed in the minimum representation, plus the sink. For clarity, S -vector entries S_I will be separated by a semicolon whenever the cardinality of I increases.

At $n = 1$ there is a single extreme ray with minimum realization the Bell pair in Figure 1,

$$S_{(1,1,1)} = (1). \tag{B.4}$$

The $n = 2$ cone has just the length-3 orbit of zero-lifts of the Bell-pair extreme ray $(1, 1, 1)$. For $n = 3$, the Bell-pair zero-lift now gives an orbit of 6 extreme rays. A new totally symmetric extreme ray appears. It has a star-graph minimum realization shown in Figure 1 and reads

$$S_{(3,2,1)} = (1, 1, 1; 2, 2, 2; 1). \tag{B.5}$$

Lifting to $n = 4$ we get orbits of 10 extreme rays from $(1, 1, 1)$ and another 5 from $(3, 2, 1)$. A genuinely new length-5 orbit of extreme rays appears,

$$S_{(4,2,1)} = (1, 1, 1, 1; 2, 2, 2, 2, 2; 3, 3, 3, 3; 2), \tag{B.6}$$

which again has a star graph as minimum realization, as shown in Figure 1.

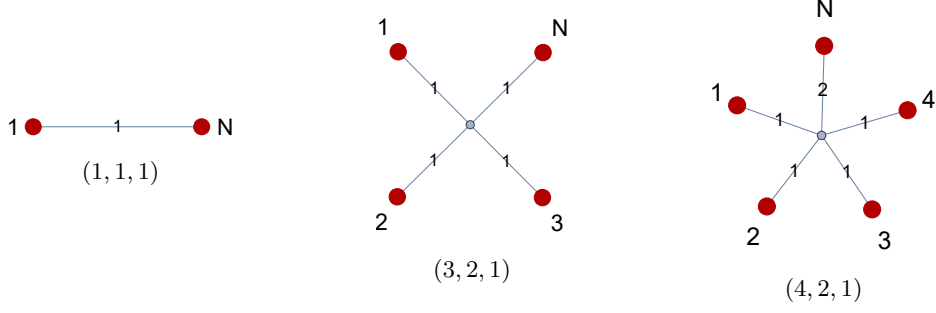


Figure 1: Minimum realizations for extreme rays in each orbit of H_n for $n \leq 4$.

At $n = 5$, lifted extreme rays become a minority. Extreme rays $(1, 1, 1)$, $(3, 2, 1)$ and $(4, 2, 1)$ respectively zero-lift to orbits of lengths 15, 15 and 30, totaling just 60 extreme rays. It turns out H_5 has 2267 in total, so all the others are genuinely new ones. They fall into 16 orbits, which we now present by increasing number of bulk vertices needed in their minimum realization. There are 4 distinct orbits of extreme rays realizable in a star graph,

$$\begin{aligned}
S_{(5,2,1)} &= (1, 1, 1, 1, 1; 2, 2, 2, 2, 2, 2, 2, 2, 2, 2; 3, 3, 3, 3, 3, 3, 3, 3, 3, 3; 2, 2, 2, 2, 2; 1), \\
S_{(5,2,2)} &= (1, 1, 1, 1, 1; 2, 2, 2, 2, 2, 2, 2, 2, 2, 2; 3, 3, 3, 3, 3, 3, 3, 3, 3, 3; 4, 4, 4, 4, 4; 3), \\
S_{(5,2,3)} &= (1, 1, 1, 1, 2; 2, 2, 2, 3, 2, 2, 3, 2, 3, 3; 3, 3, 4, 3, 4, 4, 3, 4, 4, 4; 4, 3, 3, 3, 3; 2), \\
S_{(5,2,4)} &= (1, 1, 1, 2, 2; 2, 2, 3, 3, 2, 3, 3, 3, 3, 4; 3, 4, 4, 4, 4, 5, 4, 4, 5, 5; 5, 5, 4, 4, 4; 3),
\end{aligned} \tag{B.7}$$

with respective orbit lengths 1, 6, 15 and 60. They can all be represented on the star graph shown in Figure 2(1), with appropriate weight assignments as specified in Table 3. There are 6 orbits which require 2 bulk vertices,

$$\begin{aligned}
S_{(5,3,1)} &= (1, 1, 1, 1, 1; 2, 2, 2, 2, 2, 2, 2, 2, 2, 2; 1, 3, 3, 3, 3, 3, 3, 3, 3, 3; 2, 2, 2, 2, 2; 1), \\
S_{(5,3,2)} &= (1, 1, 1, 1, 1; 2, 2, 2, 2, 2, 2, 2, 2, 2, 2; 2, 2, 2, 3, 3, 3, 3, 3, 3, 3; 2, 2, 2, 2, 2; 1), \\
S_{(5,3,3)} &= (1, 1, 1, 1, 2; 2, 2, 2, 3, 2, 2, 3, 2, 3, 3; 3, 3, 2, 3, 4, 4, 3, 4, 4, 4; 4, 3, 3, 3, 3; 2), \\
S_{(5,3,4)} &= (1, 1, 2, 2, 2; 2, 3, 3, 3, 3, 3, 3, 4, 4, 4; 4, 4, 4, 3, 3, 5, 5, 5, 5, 4; 4, 4, 4, 3, 3; 2), \\
S_{(5,3,5)} &= (2, 2, 2, 2, 3; 4, 4, 4, 5, 4, 4, 5, 4, 5, 5; 4, 6, 5, 6, 5, 7, 6, 7, 7, 7; 6, 5, 5, 5, 5; 3), \\
S_{(5,3,6)} &= (3, 3, 3, 3, 3; 6, 6, 6, 6, 6, 6, 6, 6, 6, 6; 5, 7, 7, 7, 7, 9, 9, 9, 9, 9; 6, 6, 6, 6, 6; 3),
\end{aligned} \tag{B.8}$$

with respective orbit lengths 10, 60, 90, 180, 360 and 90. These can be represented on graphs in Figures 2(2) to 2(5) following Table 3. There are 6 orbits which require 3 bulk vertices,

$$\begin{aligned}
S_{(5,4,1)} &= (1, 1, 1, 1, 1; 2, 2, 2, 2, 2, 2, 2, 2, 2, 2; 2, 2, 2, 2, 3, 3, 3, 3, 3, 3; 2, 2, 2, 2, 2; 1), \\
S_{(5,4,2)} &= (1, 1, 1, 1, 1; 2, 2, 2, 2, 2, 2, 2, 2, 2, 2; 2, 2, 3, 3, 2, 3, 3, 3, 3, 3; 2, 2, 2, 2, 2; 1), \\
S_{(5,4,3)} &= (2, 2, 2, 2, 3; 4, 4, 4, 5, 4, 4, 5, 4, 5, 5; 4, 6, 5, 6, 7, 5, 6, 7, 7, 7; 6, 5, 5, 5, 5; 3), \\
S_{(5,4,4)} &= (3, 3, 3, 3, 3; 6, 6, 6, 6, 6, 6, 6, 6, 6, 6; 5, 7, 7, 7, 9, 9, 9, 7, 9, 9; 6, 6, 6, 6, 6; 3).
\end{aligned} \tag{B.9}$$

with respective orbit lengths 180, 60, 360 and 360. These are realizable in graphs in Figures 2(6) to 2(8) following Table 3.

Finally, there is an orbit of length 360 with 4 bulk vertices,

$$S_{(5,5,1)} = (3, 3, 3, 3, 3; 6, 6, 6, 6, 6, 6, 6, 6, 6, 6; 5, 7, 7, 7, 9, 7, 9, 9, 9, 9; 6, 6, 6, 6, 6; 3), \tag{B.10}$$

and another one of length 15 with 5 bulk vertices,

$$S_{(5,6,1)} = (1, 1, 1, 1, 1; 2, 2, 2, 2, 2, 2, 2, 2, 2, 2; 2, 2, 3, 3, 2, 2, 3, 3, 3, 3; 2, 2, 2, 2, 2; 1). \tag{B.11}$$

These are respectively realizable in graphs in Figures 2(7) and 2(8) following Table 3.

In summary, H_5 consists of 2267 extreme rays in 19 orbits, 2207 of which lie in 16 orbits new to $n = 5$. Note that apart from the Bell pair $(1, 1, 1)$ in Figure 1, there are no edges between terminals in any of the minimum extreme-ray representations. Each is planar except for $(5, 6, 1)$ in Figure 2(8), which can be embedded on a torus. Terminals have degree at most 3.

C Miscellaneous examples

Convexity of $H_{N,n}^+$ and $H_{N,n}$: For $n = 5$, consider extreme rays $S_{(5,2,2)}$ and the zero-lift of $S_{(3,2,1)}$, both of which are realizable in K_7 . Using the ILP method in Section 5 we can determine that their sum is not. Therefore, neither $H_{7,5}^+$ nor $H_{7,5}$ is convex without the convex operator applied. The minimum realization of their sum is in K_8 , and has edges $\{(1, 6), (2, 6), (3, 6), (4, 7), (5, 7), (6, 7), (7, 8)\}$ with respective weights $\{2, 2, 2, 1, 1, 4, 4\}$.

Extreme rays of $P_{N,n}$ and $H_{N,n}$: For $n = 5$ in K_9 , consider these three feasible (S, w) pairs:

$$\begin{aligned} S^1 &= (3, 4, 3, 3, 3; 7, 6, 6, 6, 7, 7, 7, 6, 6, 6; 6, 8, 6, 9, 9, 7, 8, 8, 8, 9; 5, 5, 5, 6, 5; 2), \\ S^2 &= (1, 2, 1, 1, 1; 3, 2, 2, 2, 3, 3, 3, 2, 2, 2; 2, 2, 2, 3, 3, 3, 2, 2, 2, 3; 1, 1, 1, 2, 1; 0), \\ S^3 &= (2, 2, 2, 2, 2; 4, 4, 4, 4, 4, 4, 4, 4, 4, 4; 4, 6, 4, 6, 6, 4, 6, 6, 6, 6; 4, 4, 4, 4, 4; 2), \\ w^1 &= (0, 0, 0, 0, 2, 1, 0, 0; 0, 0, 0, 3, 1, 0, 0; 0, 0, 2, 0, 1, 0; 0, 1, 1, 1, 0; 1, 2, 0, 0; 0, 1, 0; 1, 0; 2), \\ w^2 &= (0, 0, 0, 0, 1, 0, 0, 0; 0, 0, 0, 2, 0, 0, 0; 0, 0, 1, 0, 0, 0; 0, 1, 0, 0, 0; 1, 0, 0, 0; 0, 0, 0; 0, 0; 0), \\ w^3 &= (0, 0, 0, 0, 1, 0, 1, 0; 0, 0, 0, 0, 2, 0; 0, 0, 0, 1, 1, 0; 0, 1, 1, 0, 0; 2, 0, 0, 0; 1, 1, 0; 1, 2; 0). \end{aligned}$$

Here (S^1, w^1) is an extreme ray of $P_{9,5}$. However, its S coordinates have $S^1 = S^2 + S^3$, so the latter cannot be an extreme ray of $H_{9,5}$ and hence of H_5 either (cf. Theorem 2(b)).

Extreme Ray (\cdot, \cdot, \cdot)	Graph #	Terminal Edges					Edge Weights																		
		N	1	2	3	4	5	w_N	w_1	w_2	w_3	w_4	w_5	w_6	w_7	w_8	w_9	w_{10}	w_{11}	w_{12}	w_{13}	w_{14}	w_{15}		
(5, 2, 1)	1						1	1	1	1	1	1													
(5, 2, 2)	1						3	1	1	1	1	1													
(5, 2, 3)	1						2	1	1	1	1	2													
(5, 2, 4)	1						3	1	1	1	2	2													
(5, 3, 1)	2						1	1	1	1	1	1	1												
(5, 3, 2)	3						2	2	2	1	1	1	1	1	1	1									
(5, 3, 3)	2				w_5	w_3	2	1	1	2	1	1	2												
(5, 3, 4)	4						2	1	1	2	1	1	1	1	1										
(5, 3, 5)	3	w_1	w_N	w_4		w_2	2	3	2	1	1	2	1	1	1	1									
(5, 3, 6)	5						3	3	2	2	2	2	2	1	1	1	1	1							
(5, 4, 1)	6						2	1	2	1	1	1	1	1	1	1	1	1	1	1	1	1			
(5, 4, 2)	7						1	2	1	1	2	2	1	1	1	1	1	1	1	1	1				
(5, 4, 3)	7	w_1	w_N	w_3	w_4	w_2	1	3	1	1	2	3	2	1	1	1	1	1	1	1	1				
(5, 4, 4)	8						3	2	2	1	2	2	1	1	1	1	1	1	1	1	1	1	1	1	1
(5, 5, 1)	9						3	3	3	1	1	3	2	2	1	1	1	1	1	1	1	1	1	1	1
(5, 6, 1)	10						1	1	1	1	1	1	1	1	1	1	1	1	1	1	1	1	1	1	1

Table 3: Extreme ray vs graph cross reference table for Figure 2. The columns under “Terminal Edges” specify which edge w_j is incident to each extended terminal $i \in [5; N]$, with a blank entry indicating $j = i$. Edge weights give all extreme rays listed throughout Appendix B.2, up to overall scaling.

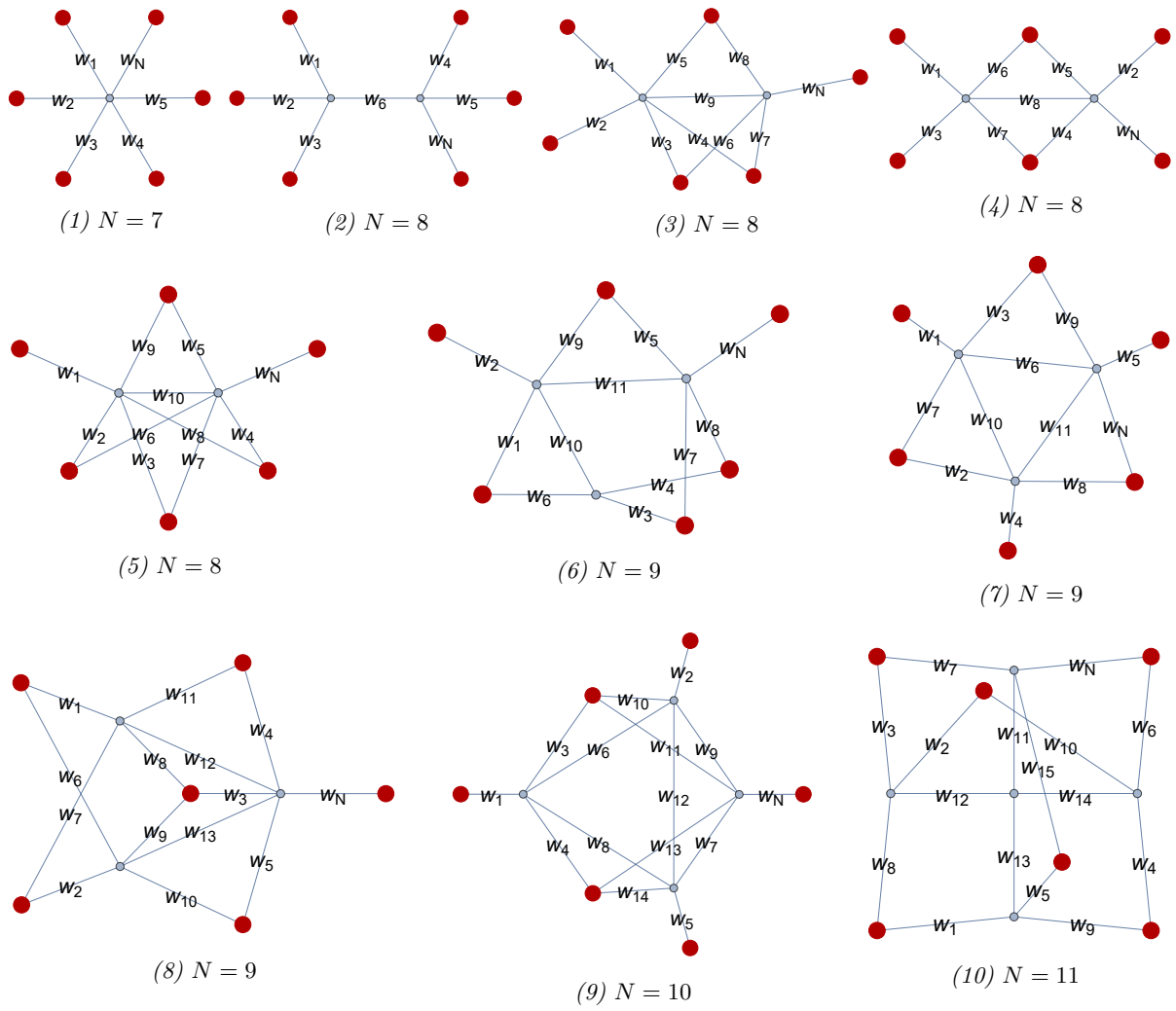


Figure 2: Minimum realizations for extreme rays which are new for H_5 .